LTRR-SRP II

The Current Drought In Context: A Tree-Ring Based Evaluation of Water Supply Variability for the Salt-Verde River Basin

Final Report

July 2008

A Collaborative Project between The University of Arizona's Laboratory of Tree-Ring Research & The Salt River Project

David M. Meko & Katherine K. Hirschboeck
Laboratory of Tree-Ring Research
The University of Arizona

With the assistance of: Christine Hallman, Kiyomi Morino, Ela Czyzowska & Ashley Coles
Laboratory of Tree-Ring Research, The University of Arizona
&
Salt River Project / Water Resource Operations

The Laboratory of
Tree-Ring Research
THE UNIVERSITY OF ARIZONA.

SRP
Delivering more than power.™

*This report is dedicated
to the memory of
Dallas Reigle of SRP*

A Collaborative Project Involving
The Laboratory of Tree-Ring Research (LTRR) & The Salt River Project (SRP)

THE CURRENT DROUGHT IN CONTEXT: A TREE-RING BASED EVALUATION OF WATER SUPPLY VARIABILITY FOR THE SALT-VERDE RIVER BASIN

David M. Meko & Katherine K. Hirschboeck
Laboratory of Tree-Ring Research, The University of Arizona

FINAL REPORT [1]
July 31, 2008

ABSTRACT

Tree-ring cores collected in 2005 were combined with existing collections to produce a new tree-ring based streamflow reconstruction for the Salt+Verde+Tonto watershed covering the period 1330-2005. The new reconstruction reveals that recent individual years (1996 and 2002) were unsurpassed in terms of low flow, with 2002 having an unprecedented number of locally absent (missing) rings. The multi-year persistence of the current drought of 1996-2006 was not unprecedented in the reconstruction. The median interval between "drought relieving" wet years was 3 years, the longest interval was 22 years (1382-1403) and 28 other droughts were more continuously severe in terms of "consecutive years below normal." The overall conclusion is that despite the single-year severity of 1996 and 2002, the current drought is by no means unique in the long-term record.

INTRODUCTION

The purpose of this project was to update the tree-ring reconstructions of annual streamflow of the Salt-Verde-Tonto Basin through the period of the current (and ongoing) drought of the late-1990s and early 2000's. The project was designed to build on the work and results of our previous project with SRP (LTRR-SRP I) which compared the Upper Colorado River basin and the Salt-Verde-Tonto River basin with respect to years with extreme high flow and low flow over the period 1521-1964. This follow-up project covered the period of the most recent ongoing drought (through 2004) and the subsequent wet winter of 2004-05 which helped to ameliorate the effects of the ongoing drought. The project also examined the degree to which variations in seasonal precipitation could be identified in the tree-ring record by examining partial-width measurements in the tree rings (earlywood and latewood). The overall goal of the project was: **to place the most recent droughts of the instrumental period (post -1960s) into a long term, historical context linked to climatic variability.**

The central questions guiding the research were: **How have tree rings recorded the recent severe drought years of the 1990s and early 2000's and how does this current drought compare with past droughts reconstructed by tree rings?** Specifically the project objectives were:

I. To recollect tree ring cores from selected sites in the Salt-Verde watershed in order to update the tree-ring chronologies in the basin through summer 2005.

II. To measure earlywood and latewood widths from the new chronologies in order to analyze the influence of the winter vs. summer component of precipitation on tree growth in the Salt-Verde Basin and to extract seasonal information on drought history and streamflow.

---

[1] This report summarizes the results of work completed by the University of Arizona's Laboratory of Tree-Ring Research (LTRR) at the request of the Salt River Project (SRP) during the period 2005-2007. The project results also include a companion website containing the appendices, relevant data, and related links. It can be found at the following URL: http://fp.arizona.edu/kkh/srp2.htm

III. To re-calibrate, update, and analyze the Salt-Verde Basin tree-ring reconstructions of streamflow using the new collections, chronologies, and seasonally separated ring width information in order to place the most recent drought and high flow extreme years in the context of the entire record, including present and past climatic variability.

IV. To define the relationship between tree-ring data and winter precipitation (specifically snow depth, snow extent, and snow water equivalent) through both ground-based and remotely sensed observations and use this information to develop a tree-ring-based historical snowpack assessment.[2]

V. To integrate the results of objectives (I) through (IV) into a report that links the long-term tree-ring reconstruction of the Salt-Verde streamflow with recent observations of gaged streamflow, seasonal precipitation, snow cover [2] and climate variability.

The project generated a large volume of data, documentation, statistics, and analytical results presented in both tables and figures. The bulk of this information is included in the appendices which can be found on the companion Project Website.

An overview of the project methodology is shown at right. The work accomplished and the project findings will be presented in this report via a question/answer format that should be broadly applicable for use in a variety of settings such communicating with water managers, water resource scientists, water consumers, legislators and the general public.

Sections to follow are:

(1) Data Overview
(2) Reconstruction Models
(3) Reconstruction Results
(4) Climatic Context and Discussion
(5) Summary and Conclusions

MAIN PROJECT ACTIVITIES

1. **UPDATING TREE-RING CHRONOLOGIES** – Field collections and laboratory analysis to develop chronologies in the Salt-Verde basin with data through growth year 2005

2. **NEW STREAMFLOW RECONSTRUCTION** – Analysis of the new tree-ring chronologies to place the most recent drought in a long-term context

3. **EW-LW EVALUATION** – Exploration of the seasonal precipitation signal in separate measurement of earlywood and latewood width measurements

4. **CLIMATIC ANALYSES** – Synoptic dendroclimatology studies of observed record to better interpret the reconstructed record

---

Additional documentation is included in the following appendices: Appendix 1 - Listing of Observed Water-Year Average Flows, Appendix 2- Field Collections and Ring-Width Data, Appendix 3 - Chronology Development, and Appendix 4 - Reconstruction Method.

1 – DATA OVERVIEW

The main conclusions of this project are based on a tree-ring reconstruction of annual (water-year, WY) streamflow summed over the months from October-September. Because most existing tree-ring records for the study region had been collected before 1990, new field collections were essential for placing the current drought in context.

(1-a)   *What river basins and streamflow gages were reconstructed?*

Table 1 lists the 4 rivers / gages for which streamflow reconstructions were completed. **Appendix 1** provides additional information on the gages used, the data sources, and the observed water-year average flows for these rivers.

---

[2] The snow study (Objective IV) is part of Ela Czyzowska's PhD dissertation still in progress. Its final results are forthcoming and will not be addressed here. A report will be provided to SRP upon completion of the dissertation.

Table 1. Statistics of observed flows in million acre-feet (MAF) for gages reconstructed

L[1]	River/gage[2]	Coverage[3]	Statistics[4]			
			Mean	Std dev	cv	skew
a	Salt + Verde + Tonto	1914-2007	1.196	0.877	0.73	1.54
b	Salt + Tonto	1914-2007	0.744	0.577	0.78	1.58
c	Verde	1914-2007	0.452	0.318	0.70	1.47
d	Gila nr head of Safford Valley	1915-2006	0.360	0.317	0.88	2.01

[1] Letter code for gage (used throughout report)
[2] Name of river or gage (see Appendix 1 for details)
[3] Start and end year of water-year totals used for statistics
[4] Mean, standard deviation, coefficient of variation and skewness of water-year-average flows in million acre-feet (maf)

The rivers and approximate gage locations are shown on the map in **Figure 1.** Analysis in this report focuses on a reconstruction for aggregate flow of the Salt, Verde and Tonto Rivers (SVT). [3]
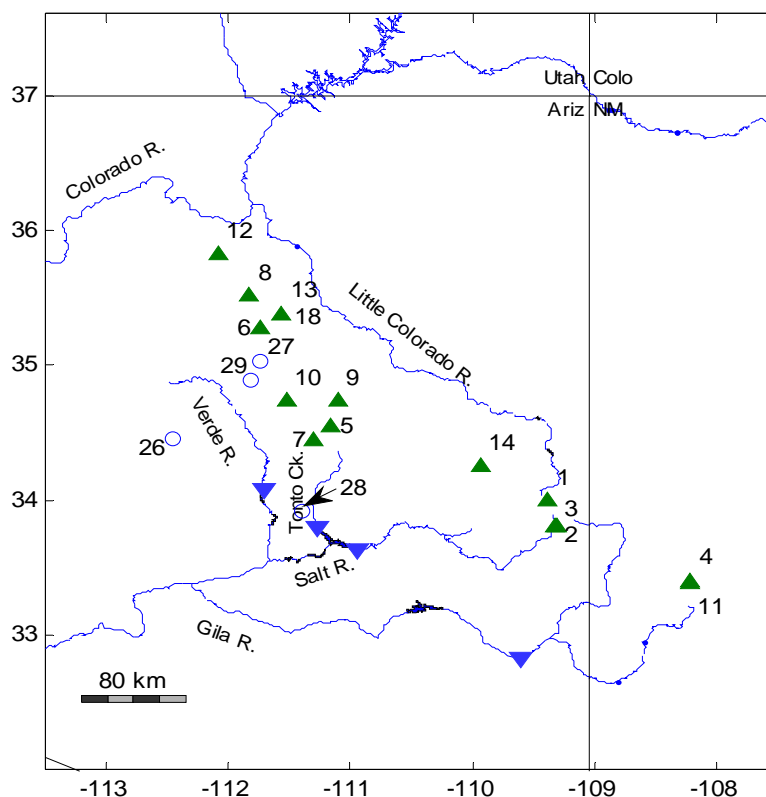

Figure 1. Map showing locations of gages reconstructed and new tree-ring collections.

Approximate gage locations are shown by blue inverted triangles, and tree-ring collection sites (fall, 2005) by green triangles and open circles. Main reconstruction for this report is SVT (Salt+Verde+Tonto), which is the sum of the three northernmost rivers. Some closely spaced tree-ring sites (e.g., 4, 11) are represented by a single symbol. Open circles mark locations where sites were evaluated but only a few or no samples taken.

---

[3] Reconstructions of annual (water-year) flow for the Salt+Tonto, Verde, and Gila Rivers are available on request from the authors.

(1-b)   *What information obtained from tree rings is used to link tree growth with streamflow?*

For this study the tree-ring information on streamflow comes from the width of the annual ring.[4] In a typical dendrohydrologic study, the ring widths from 10-30 trees at a site for several sites are reduced to dimensionless indices, or "site chronologies," which are then linked statistically to streamflow variations.   The tree-ring index can be regarded as the proportion of normal growth in each year such that values above 1.0 represent higher than normal growth and values below 1.0 represent lower than normal growth (see **Figure 2**). The minimum index that can occur theoretically is zero, or no growth in a given year.
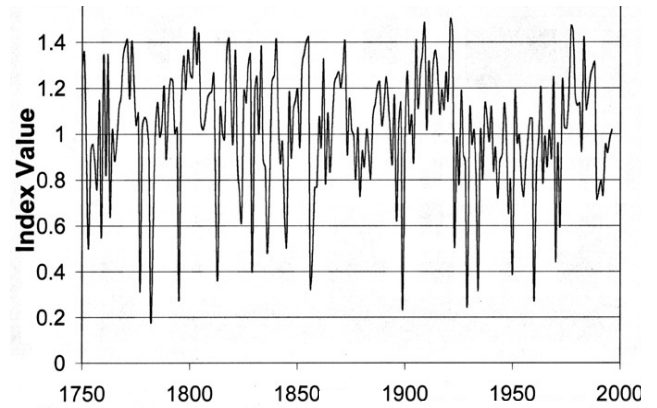

Figure 2. Example of a tree-ring site chronology with standardized index values representing ring widths

(1-c)   *Why should there be a relationship between streamflow and tree growth in the arid and semi-arid western United States?*

For properly sampled trees from semi-arid sites, growth can be limited by water stress resulting from a combination of low soil moisture and high evaporative demand. Hot, dry conditions also reduce the runoff available to rivers and streams, as runoff is the difference of precipitation and evapotranspiration. Streamflow represents regionally integrated runoff. Hence both trees and streams can respond to weather and climate patterns that produce sustained drought conditions (**Figure 3**). Snowpack can impact both timing and amount of runoff, and can also affect tree growth. In the project study area, the snow that falls in the winter *prior* to a tree's growing season is reflected in the tree's growth in spring and summer via soil moisture storage. The melting snowpack can mitigate water stress in the trees by making water available to the roots as conditions warm up through the spring.

Figure 3 -- Why tree growth and streamflow variations are correlated (see Meko et al. 1995)

(1-d)   *What's the benefit of using tree-rings to study past streamflow variation?*

Gage records for the Salt-Verde River system are some of the longest in the United States, yet they represent only a short segment of these rivers' long-term natural variability. Droughts and floods can have devastating impacts on people, but because they are rare events, even 100 years of instrumental streamflow records may not be long enough to capture the range of possible extreme streamflow episodes. Climate-sensitive tree-ring records can extend the record of climate and hydrologic variability back many centuries to provide important information unavailable from the gaged record. In one of the first statistical streamflow reconstructions from tree rings, Stockton (1975), Stockton and Jacoby (1976) demonstrated how unusually wet the early 20th century was in the Colorado River in comparison to the long-term mean. Water supply planning decisions made on the basis of unusually wet or dry episodes of a river's history may not properly represent the true nature of the supply.

---

[4] Chemical and other physical properties of rings can also be used for hydrologic information. Partial-width (earlywood and latewood) measurements, for example, were investigated in an exploratory part of the study, but were not used in the streamflow reconstruction.

(1-e)   *How were the tree-ring sites selected for the analysis?*

The study used a combination of updated, new and pre-existing tree-ring chronologies. A large part of the effort was the updating of chronologies in or near the Salt-Verde watershed. Field trips in fall of 2005 were made to 18 different site locations, and resulted in 14 tree-ring site chronologies complete through the 2005 growth ring (**Table 2, Figure 1**). The sites visited were judged as especially promising based on past tree-ring studies in the basin. Two of the sites yielding chronologies (4-Wolf Head Draw and 5-East Clear Creek) had not been previously collected. At the other sites visited in 2005, we took advantage of earlier collections by merging their archived ring-width records with our updated measurements. Besides the new and updated chronologies, we used 11 additional pre-existing chronologies notable for their length and climatic sensitivity.

Table 2. Tree-ring sites for new field collections

N^1	Site Name	$Spec^2$	Location[3]			T^4	Date[5]	N_T^6
			Lat	Lon	El (ft)			
1	Wahl Knoll	PSME	34.00	-109.39	9625	P	11-19-05	18
2	Black River Fir	PSME	33.81	-109.32	6754	P	09-23-05	20
3	Black River Pine	PIPO	33.81	-109.32	7921	P	11-17-05	25
4	Wolf Head Draw Fir	PSME	33.40	-108.22	6593	P	10-13-05	8
5	East Clear Creek	PIPO	34.55	-111.16	6706	T	11-11-05	19
6	Gus Pearson	PIPO	35.27	-111.74	7423	T	10-27-05	30
7	Mogollon Rim West Fir	PSME	34.44	-111.29	7511	T	11-03-05	5
8	Slate Mountain	PIPO	35.52	-111.83	7027	T	10-28-05	31
9	Jacks Canyon	PIED	34.75	-111.11	6303	T	11-10-05	17
10	Rocky Gulch	PIPO	34.73	-111.52	6453	T	11-10-05	22
11	Black Mountain Lookout	PSME	33.38	-108.22	8692	T	10-13-05	15
12	Red Butte	PIED	35.83	-112.08	6332	T	10-28-05	16
13	Robinson Mountain	PIPO	35.38	-111.56	7313	T	10-27-05	30
14	Sitgreaves Gravel Pit	PIPO	34.25	-109.94	6740	T	09-24-05	24
a	Oak Creek Canyon	PSME	35.03	-111.74	5904	N	10-21-05	4
b	Wolf Creek Campground	PIPO	34.45	-112.45	5871	N	10-21-05	4
c	Dry Creek	PIED	34.89	-111.82	4526	N	10-21-05	0
d	Oak Spring Canyon	PIPO	33.92	-111.40	6199	N	10-19-05	0

[1] N = map number or letter (see Figure 1)
[2] Species: PSME = *Pseudotsuga menziesii*; PIPO = *Pinus ponderosa* PIED = *Pinus edulis*
[3] Location = latitude and longitude in decimal degrees; elevation in ft
[4] T = type of chronology developed (P=partial width and total width, T=total width only, N=none)
[5] Date = month-day-year of field collection
[6] N_T: number of trees sampled : Sites a & b = exploratory samples were taken; Sites c & d = sites visited but no samples taken

The 25 resulting chronologies are plotted in **Figure 4** and listed in **Table 3**. All of these chronologies have data as recent as 1983. That end date was dictated by our preference to have a reasonably long period for calibration with the flow record, which beings in 1914. Our selection of chronologies was also guided by a need for a well-replicated network to sample such noted events as the late-1500s megadrought (Stahle et al. 2000) and the "Pueblo" drought, which occurred in the late 1660s (Smith and Stockton 1981).   Three different species are represented in the 25-site network (Table 3). Elevations of sites range from about 6,200 ft to 9,500 ft, and starting year of chronologies from 1100 to 1736.[5]

---

[5] The earliest available tree-ring data at some of the sites pre-dates 1100, but our data processing (e.g., detrending) began with a networked of ring-width series truncated at 1100.
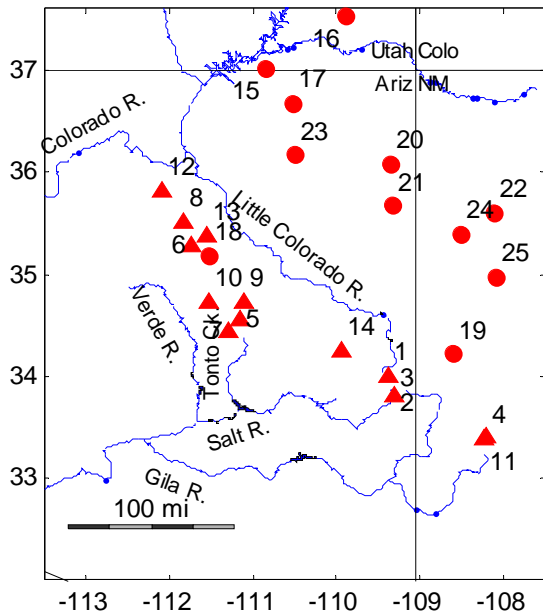
Figure 4. Map showing locations of 25 tree-ring chronologies used in reconstruction models.

Chronologies are pre-existing (circles), or from fall 2005 field collections (triangles). Some closely spaced chronologies represented by single symbol. Sites numbered as in Table 3.

Table 3. Tree-ring chronologies used in flow reconstruction

N [1]	Site [2]	File [3]	Species [4]	Location [5]			Period [6]	PI [7]
				Lat	Lon	El (m)		
1	Wahl Knoll,	whkwt2	PSME	34.0	-109.4	9512	1435-2005	d
2	Black River	brfwt1	PSME	33.8	-109.3	6757	1598-2005	d
3	Black River	brpwt1	PIPO	33.8	-109.3	7921	1598-2005	d
4	Wolf Head D	wlfwt1	PSME	33.4	-108.2	6593	1736-2005	d
5	East Clear	eccwt1	PIPO	34.5	-111.2	6704	1694-2005	d
6	Gus Pearson	guswt1	PIPO	35.3	-111.7	7423	1583-2005	d
7	High View P	hvwwt1	PSME	34.4	-111.3	7872	1595-2005*	d
8	Slate Mount	slawt1	PIPO	35.5	-111.8	6986	1634-2005	d
9	Jacks Canyon	jkcwt1	PIED	34.7	-111.1	6298	1686-2005	d
10	Rocky Gulch	rghwt1	PIPO	34.7	-111.5	6429	1694-2005	d
11	Black Mount	bkmwt1	PSME	33.4	-108.2	8856	1327-2005	d
12	Red Butte,	redwt1	PIED	35.8	-112.1	6298	1478-2005	d
13	Robinson Mo	robwt1	PIPO	35.4	-111.6	7314	1619-2005	d
14	Sitgreaves	sgpwt1	PIPO	34.3	-109.9	6757	1640-2005	d
15	Navajo Moun	nvn90	PIED	37.0	-110.8	7498	1330-1989	a
16	Kane Spring	nat90	PIED	37.5	-109.9	6448	1361-1988	a
17	Betatakin C	bet90	PSME	36.7	-110.5	6701	1306-1989	a
18	Walnut Canyon	wcpwt1	PIPO	35.2	-111.5	6799	1451-1987	b
19	Agua Fria	agfwt1	PIED	34.2	-108.6	7298	1496-1987	b
20	Spider Rock	cdcwt1	MIX	36.1	-109.3	6199	1399-1989	a
21	Cross Canyon	crswt1	PIPO	35.7	-109.3	7200	1541-1989	a
22	Satan Pass	spswt1	PSME	35.6	-108.1	7498	1410-1990	a
23	Upper Dinne	dinwt1	PIED	36.2	-110.5	6298	1410-1983	a
24	Turkey Spri	tspwt1	PIED	35.4	-108.5	7797	1490-1985	a
25	El Malpais	nm572_b	PSME	35.0	-108.1	7947	1100-1990	c

[1] Site number
[2] Site name, truncated
[3] Prefix of ring-width-list (rwl) file
[4] Species code: PIED=*Pinus edulis*; PIPO=*Pinus ponderosa*; PSME=*Psuedotsuga menziesii*; MIX=mix of two or more of the preceding species
[5] Latitude and longitude in decimal degrees, elevation in feet above sea level
[6] Start and end year of chronology, after trimming off all data preceding 1100

[7] Code cross-referenced to Principal Investigator responsible for chronology collection: (a) & (b) Jeff Dean and collaborators from Southwest Archaeology Project, (c) Henri Grissino-Mayer, (d) David Meko --- primarily updates of chronologies previously collected by researchers from Laboratory of Tree-Ring Research (LTRR)

(1-f)   *What were the different sources of the tree-ring data?*

Tree-ring data were obtained from four sources: (1) new and updated collections from fieldwork in fall 2005; (2) The International Tree-ring Databank (ITRDB) which is the major repository of tree-ring data in North America; (3) The Laboratory of Tree-Ring Research (LTRR) database of the Southwest Archaeology Project, which has developed a high-quality set of living-tree chronologies paired with ring-width records from archaeological structures.   Several of the existing chronologies from the different sources had previously been used in studies of spatial patterns of drought (Meko et al. 1993; Cook et al. 1999; Cook et al. 2004). Merged living-tree and archaeological-sample tree-ring records from the Southwest Archaeology project have previously been used in a 1500-year reconstruction of annual streamflow of various rivers in Arizona (Graybill et al. 2006). We restricted our use of these data to the living-tree portions, as the archaeological samples are from unknown hydrologic settings.

(1-g)   *How did you remove age-trend from the tree-ring measurements?*

The starting data for a tree-ring site were the dated and measured ring widths. We processed these uniformly to produce "residual" chronologies, defined as dimensionless tree-ring indices adjusted for removal of autocorrelation (Cook and Kairiukstis 1990). The main steps in processing are 1) fit a smooth line defining the "age-trend" or "size-trend" to each ring-width series, 2) compute the core index as the ratio of measured ring width to the value of the smooth curve, 3) remove the persistence from the resulting "standard" core indices (Cook and Kairiukstis 1990) with autoregressive modeling, and 4) average the resulting residual core indices over all trees to get the residual site chronology. A cubic smoothing spline (Cook and Peters 1981) with a frequency response of 0.95 at twice the series length was used as the detrending curve for all ring-width series. In keeping with the "trend-in-mean" concept (Granger and Hatanaka 1964), this processing removes almost completely the variations at wavelengths longer than twice the sample length. Such variations cannot be distinguished statistically from monotonic trend, which is expected from geometric considerations – annual increment of growth deposited on an ever-increasing tree-diameter (Fritts 1976). More details in the chronology development are in **Appendix 3**.

2 – RECONSTRUCTION MODELS

(2-a)   *What guided the design of the streamflow reconstruction model?*

Several objectives were considered in deciding on a reconstruction procedure. The model should address the tree-ring variations of the most recent few years, as the "current drought" is a focus of the research. The model should extend back far enough in time so sample know interesting periods of anomalous climate in the western United States, such as the North American "megadrought" of the late 16th century (Stahle et al. 2000). The model should rely on as many tree-ring chronologies as possible to ensure robustness – to avoid oversensitivity to possible irregular responses of growth to climate at individual sites. The modeling procedure should include safeguards against over-fitting, and should be flexible to possible nonlinearity and outliers in the relationship between tree-growth and streamflow.

(2-b)   *What are the steps of the streamflow reconstruction procedure?*

The streamflow reconstruction procedure used in this study had four stages (I - IV, see **Figure 5**).   This section summarizes the procedure. More details can be found in Appendix 4.

Stage I – Selection of tree-ring chronologies. The selection of the chronologies was described in section 1e. The selection yielded a set of 25 chronologies – 14 from field collection in fall of 2005, and 11 from earlier collections (**Figure 4, Table 3**).
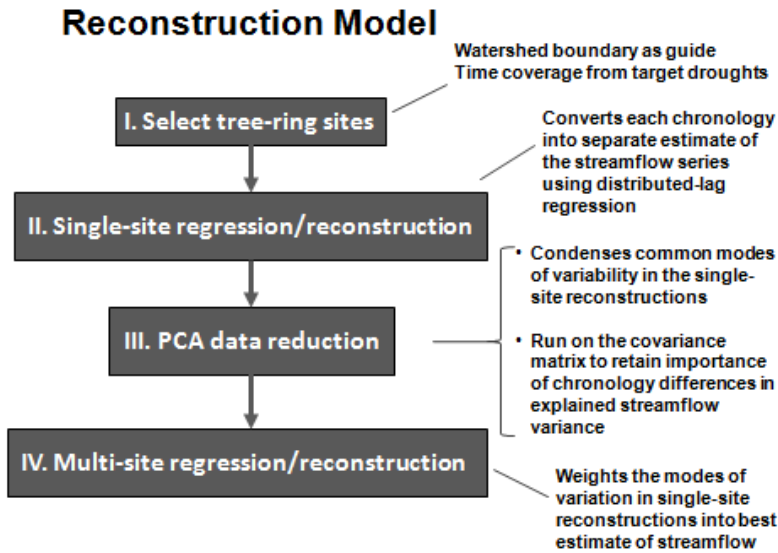
Reconstruction Model

Figure 5. Stages in the streamflow reconstruction method.

Stage II – Single-site regression/reconstruction. For each tree-ring chronology, flow was regressed on the residual site chronology in a distributed-lag model using robust regression and a linear or quadratic model to convert the chronology into an estimate of the flow series. Repetition of this procedure for each of the 25 chronologies resulted in 25 separate tree-ring reconstructions of flow, one for each chronology (see examples in **Figure 6**). In this sense each regression could be viewed as single-site reconstruction of flow. Alternatively the regression could be considered a filtering and scaling of each chronology to emphasize its flow signal.

Figure 6. Examples of single-site regression fits to scatterplots of flow on residual tree-ring chronologies.

Sites are numbered as in **Table 3**. Statistics on the fitted models are listed in **Table 4**.

- 8 -
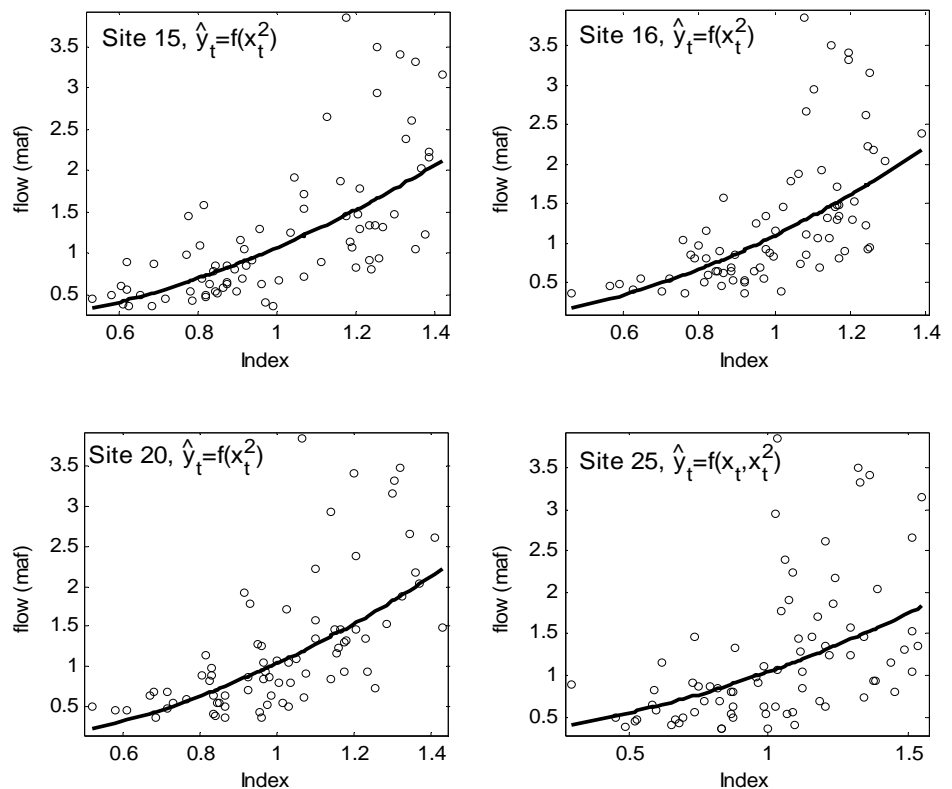
Table 4. Summary statistics for single-site regression models for the 21 chronologies with a statistically significant and stable signal for flow.

N [1]	Model [2]	Calibration [3]		Validation [4]	
		Period	R^2	$RMSE_v$	MAE_v
1	2:2000	1914-2004	0.26	0.80	0.27
2	12:0000	1914-2004	0.13	0.84	0.33
4	1:0000	1914-2004	0.11	0.84	0.29
5	1:1000	1914-2004	0.12	0.87	0.33
8	2:2000	1914-2004	0.35	0.78	0.32
9	12:0000	1914-2004	0.23	0.82	0.37
10	1:1000	1914-2004	0.25	0.81	0.28
11	2:0000	1914-2004	0.17	0.82	0.31
12	2:0000	1914-2004	0.33	0.76	0.26
14	2:0000	1914-2004	0.36	0.74	0.20
15	2:0000	1914-1989	0.46	0.66	0.30
16	2:0000	1914-1988	0.36	0.71	0.27
17	2:0000	1914-1989	0.34	0.70	0.32
18	2:0002	1914-1985	0.31	0.75	0.30
19	12:0000	1914-1987	0.19	0.81	0.43
20	2:0000	1914-1989	0.41	0.69	0.26
21	2:0000	1914-1989	0.33	0.73	0.30
22	2:0000	1914-1990	0.40	0.71	0.31
23	2:0020	1914-1982	0.62	0.60	0.31
24	2:0000	1914-1985	0.36	0.76	0.32
25	12:0000	1914-1990	0.23	0.78	0.35

[1] Site number (see Table 3 for cross-reference to site name)

[2] Code defining regression model of flow on current and lagged tree-ring index; digits before colon indicate power(s) of current-year index (e.g., 2 denotes 'squared'); columns after colon indicate powers on index at lags t-1, t-2, t+1 and t+2 years relative to the year of flow

[3] Calibration statistics: calibration period and variance-explained statistic (R^2)

[4] Validation statistics (MAF): root-mean-square error (RMSE) and median absolute error (MAE) based on leave-9-out cross-validation

Stage II serves several purposes. First is to identify chronologies not significantly related to flow. These chronologies can be eliminated from further consideration in the modeling. Second is to filter the chronologies to adjust for their variable (site-to-site) lagged relationships with flow. The lag properties of the relationship could be related to biological factors, such as multi-year needle retention by the trees. The lag properties could also arise from hydrologic factors (e.g., soil moisture carryover), or could be distortions due to the prior removal of low-order persistence from the tree-ring indices in converting them to residual site chronologies. Lags may or may not be important to the relationship between flow and chronology for any particular site. If lags are unimportant, the procedure used ensures that lags will not enter the single-site regression model. The third purpose of the single-site regression is to re-express, or scale, each chronology into flow units, such that the variance of the scaled chronology reflects the strength of its signal for flow. This scaling is convenient for later combination of the single-site reconstructions.

Two novel approaches in the regressions are the optional use of a quadratic model, and of robust regression. The quadratic model applies when the relationship between flow and tree-ring index is curvilinear, the linear model when the relationship is linear. Robust regression allows the discounting of outliers in estimating the regression. Outliers might be expected in the relationship between flow and tree-growth at any particular site, both because of nonclimatic factors that might influence growth

appreciably at times, and because in some years the precipitation or soil moisture at a particular tree-ring site may be unrepresentative of the moisture conditions of the basin.

The single-site regression modeling identified 4 chronologies to be eliminated, either because the flow signal was too weak or was unstable from the first half to the second half of the record. The number of usable chronologies was therefore reduced to 21. The procedure selected a quadratic model over a linear model for 18 of the remaining 21 chronologies (**Table 4**). Lags were relatively unimportant in the modeling. The stepwise procedure allowed lags to enter for just 6 chronologies. The coefficients on lagged terms (not shown) for those chronologies were small relative to those on the un-lagged terms. The models indicated very strong signals for flow in some individual chronologies. Percentage of flow variance explained exceeds 40 percent for 4 chronologies (**Table 4**).

Stage III – PCA Data reduction The third stage of the reconstruction procedure was principle components analysis (PCA) to combine the information from the various single-site reconstructions into single time series suitable for reconstructing flows for some specific sub-period of the tree-ring record. The time series of scores of PC1 of a group of single-site reconstructions with a common time period was defined as the new tree-ring variable.

The PCA data reduction was repeated for three different groups of chronologies with common time coverage to form three different time series of weighted tree-ring index representing different parts of the tree-ring record: A 4-chronology set covered 1330-1989; a 10-chronology set covered 1451-1982; and another 10-chronology set covered 1736-2005. The chronologies for the sub-period models are mapped in **Figure 7**.
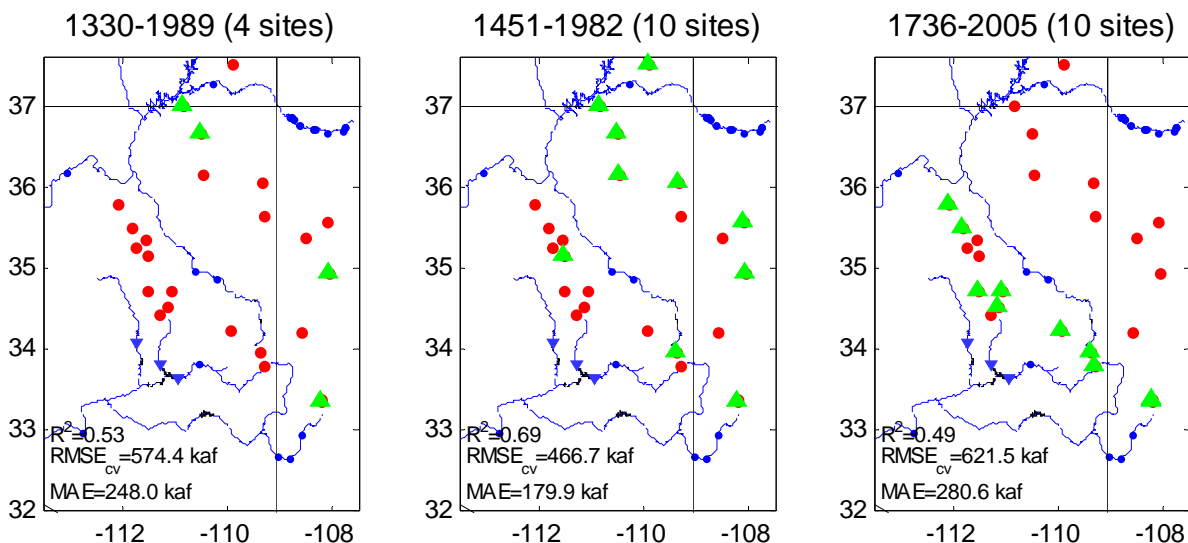

Figure 7. Maps of the chronologies used in each of the subperiod models. Green triangles indicate the chronologies used, red diamonds indicate chronologies not used, in each subperiod model.

<u>Stage IV – Loess-curve estimation and flow reconstruction.</u> The fourth stage of the reconstruction procedure was to fit a locally weighted regression (loess) to the scatterplot of flow on the weighted tree-ring series (scores of PC1 of the single-site reconstructions), and to estimate reconstructed flows by interpolating with the smoothed scatterplot. The procedure is illustrated in **Figure 8** for the sub-period model applicable to the 1451-1982 portion of the tree-ring record. Reconstructed flows for 1330-1450 and 1983-2005 periods would be estimated from similarly smoothed scatterplots tailored to the other two reconstruction sub-periods.
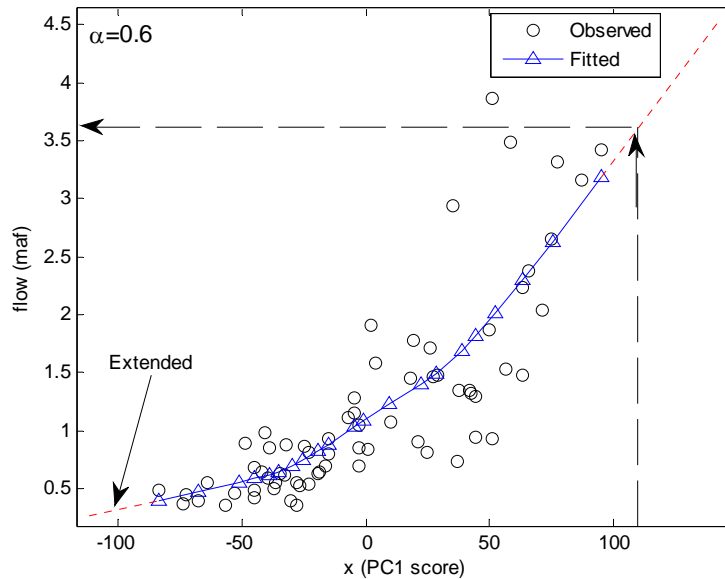
Figure 8. Loess curve used for interpolating reconstructed flow from the score of the first principle component (PC) of single-site reconstructions using the 1451-1982 sub-period model.
The scatterplot is based on the 1914-82 data. Dotted line is linear extension to allow interpolation outside the range of data in the 1914-1982 loess calibration period. Arrows illustrate using the loess curve to infer a flow of 3.6 maf from a PC#1 score of 110. Steps in reconstruction are 1) identify tree-ring chronologies covering the desired sub-period, 2) filter and scale those chronologies individually into estimates of flow, 3) run principle components analysis (PCA) on the filtered and scaled chronologies and use the scores of the first PC as the site-weighted tree-ring variable, PC1 score, 4) plot flow against PC1 score for the calibration period (1914-82), 5) smooth the scatterplot with locally weighted regression (loess) to arrive at the smooth curve shown in the figure, and 6) estimate the flow for any year of the tree-ring record by linear interpolation with the loess curve.

 (2-c)   *How uncertain are the reconstructed flows?*

The accuracy of the reconstructions interpolated from the loess plot was estimated in two ways. First is with a variance-explained statistic, computed as 1-T, where T is the ratio of the error sum-of-squares to the total sum of squares of departures from the calibration period mean of flow.
Accuracy was also estimated by a cross-validation process, which entailed: 1) leaving out 9 sequential observations, 2) fitting the loess curve to the scatterplot based on the remaining observations, 3) using the loess curve to estimate the flow central of the 9 omitted observations, 4) repeating steps 1-3 for all possible sets of 9 observations, and 5) computing validation accuracy statistics using the sequence of predictions that has been generated for the "left-out" sets. Accuracy statistics from validation included the median absolute error (MAE) as well as the root-mean-square error (RMSE) and the reduction of error statistic (RE), which has longstanding use in dendroclimatology (Gordon 1982).

Accuracy statistics for the various sub-period models are listed in **Table 5**. The calibration statistics indicate flow variance explained by the models ranges from 45 percent to 69 percent, with accuracy highest for the tree-ring sub-period 1451-1982. The RE statistics indicates this variance-explained might be biased high 2-4 percent due to model tuning. Perhaps the most practically useful measure of the uncertainty is the median absolute error of cross-validation, which ranges from 0.20 to 0.29 million acre-feet.

Table 5. Statistics of sub-period reconstruction models for Salt+Verde+Tonto flows.

N[1]	Start[2]	Calibration[3]				Validation[4]		
		Years	n	R^2	MAE	MAE	RMSE	RE
1	1330	1914-1989	4	0.53	0.28	0.29	0.60	0.50
2	1451	1914-1982	10	0.69	0.19	0.20	0.49	0.67
3	1736	1914-2004	10	0.49	0.28	0.29	0.65	0.45

[1] Sub-period model number (1 is earliest)
[2] Start year of reconstruction period
[3] Calibration statistics:
  Years=calibration period
  n = number of chronologies
  R^2 = variance-explained statistic
  MAE = median absolute error of calibration

[4] Cross-validation (leave-9-out) statistics
  MAE = median absolute error
  RMSE = root-mean-square error
  RE = reduction of error statistic

 (2-d)   *How are error bars put on the reconstructed flows?*

Error bars for estimated flows could be estimated directly from the validation RMSE if it can be assumed that the reconstruction errors follow a normal distribution (or any other distribution) whose variance is the same for all levels of reconstructed flow. But residuals analysis suggested that error variance was higher during wet years than during dry years. For that reason, we used a weighted-bootstrapping method generate error bars. The method, described in **Appendix 4**, relies on cross-validation to generate a series of calibration-period errors, and on re-sampling of the errors with weighting dependent on the size of the reconstructed flow.

(2-e)   *How well does the reconstruction track the observed flows?*

The statistics in **Table 5** clearly show that the most accurate reconstruction comes from the model using the tree-ring dataset covering 1451-1982, or the middle model. Accuracy drops off in the earlier model because only 4 chronologies cover the earlier period, and in the later model because the set of 10 chronologies that extend through 2002 does not include some extremely sensitive chronologies from the Colorado Plateau that were not part of the field-updating in 2005. Difference in tracking ability of the three reconstruction models is illustrated in the time series plots of observed and reconstructed flows in **Figure 9**. For example, the high-flow year 1941 is much more accurately depicted by model M1451 than by the other two models, which severely underestimate the wetness. In general, errors are larger for high flows than for low flows.
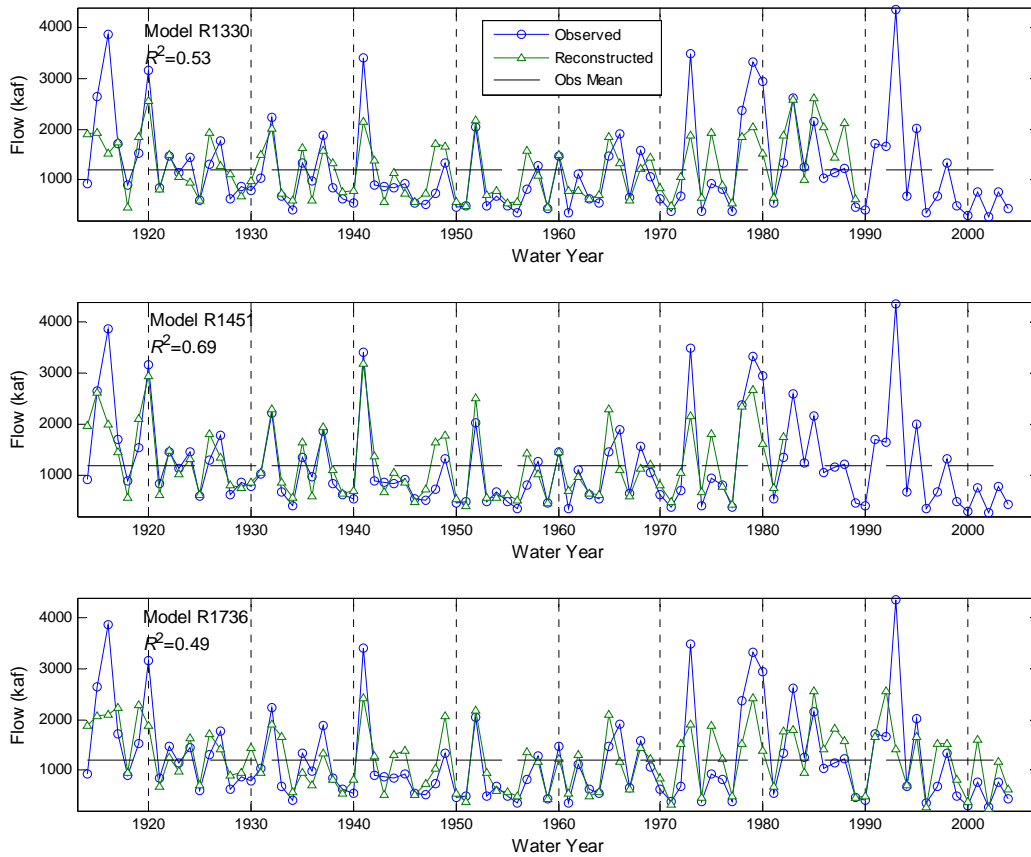
Figure 9. Time series plots showing agreement of observed and reconstructed flows for the three sub-period reconstruction models. Models are coded by the start year of the subperiod (e.g., M1451 for sub-period 1451-1982). Annotated is variance-explained statistic, R2 (see Appendix 3).

3 – RECONSTRUCTION RESULTS

(3-a)   *What does the reconstruction reveal about individual dry years during the current drought in the context of the past 6+ centuries of flow in the SVT?*

When compared with the long-term record, the "current drought" *(hereafter defined as the drought represented in the reconstruction by the period 1996-2005)* is extremely severe from the standpoint of individual years and runs of consecutive individual low flow years. **Figure 10** shows the reconstructed annual flows in the SVT for the period 1330-2005. **The years 2002 and 1996 had the lowest reconstructed individual-year annual flows in the entire 676-year record** (28% and 30% of normal, respectively, with "normal" defined as the 1914-2006 observed period). The longest stretch of <u>consecutive</u> years below normal was **5 years** and two such periods occurred: in the 1590s and 1660s.[6] The longest stretch of consecutive years below normal in the more recent interval of 1914-2005 was 4

---

[6] Note that this tally of runs depends on the choice of threshold for "normal." Medians of observed and reconstructed flow records differ for the common period of both records, which is 1914-2005. The median is lower for the observed flow record (895 kaf) compared to the reconstructed record (1059 kaf). If the more relaxed reconstructed flow median is used as a threshold for normal, the longest reconstructed run below normal is **9 years**. This occurred twice, in 1395-1403 and 1442-1450. Even with the relaxed threshold of 1059 kaf, the reconstructed flows do not contain any runs longer than 4 years in the more recent 1914-2005 period covering the current drought.

years (occurring in the 1950s). Therefore, the reconstruction indicates that **the current drought is unmatched in terms of individual-year severity, but** (as of 2006) **it has not been as continuously severe in terms of "consecutive years below normal" as 28 other droughts in the long-term record**.
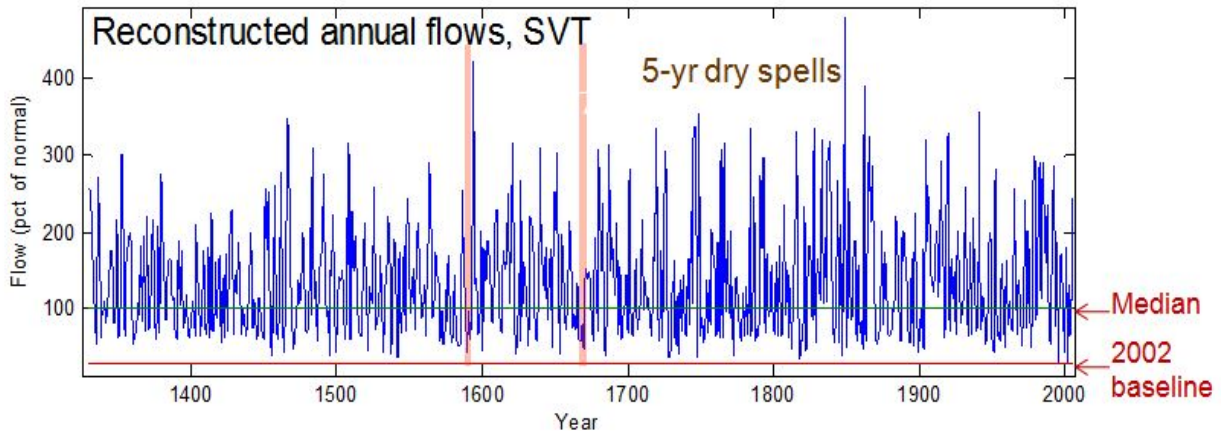

Figure 10. Reconstructed Annual Flows of Salt + Verde + Tonto (1330- 2005). Values are plotted as % of normal, with normal defined as 1914-2006 median of observed flows. The horizontal red line shows that the year 2002 experienced the lowest individual-year flow in the entire record. The second lowest flow occurred in 1996. The vertical red bars highlight the two 5-year periods that were the longest consecutive stretches of below-normal flow.

(3-b)   Do individual years during the current drought stand out in any other way in the reconstruction?

Prior to this study, a few dendrochronologists who had recently cored trees in the Southwest noted that the ring for the year 2002 was "missing," that is, the ring was locally absent at the point on the tree where it was cored. After crossdating, we confirmed the evidence of a missing 2002 ring (see **Figure 11**) in a large number of trees cored for this study. But how unusual is this for a dry year in the Southwest?
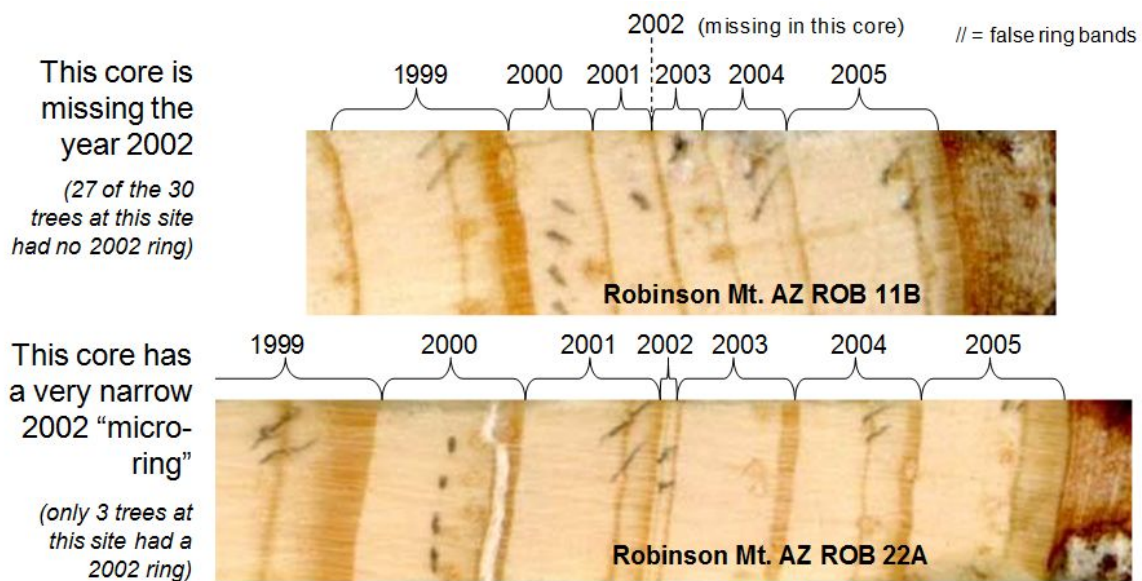
Figure 11. Example of cores with missing (locally absent) cores. The cores are from two different trees at Site 10, Robinson Mt., located near Flagstaff.

To evaluate this, we compared the number of missing rings found in the study cores in each year with the number of available cores in that year. **Figure 12** depicts the time series of this percentage, along with a

graph showing the changing number of available cores over time. **The year 2002 was unprecedented in the frequency with which the locally absent ring phenomenon occurred, with 60% of the cores missing a ring for that year!** 1996 also had a high frequency, exceeded only by the extreme dry year of 1902. This unique result augments our finding (3-a) that the current drought is unmatched in terms of individual-year severity.
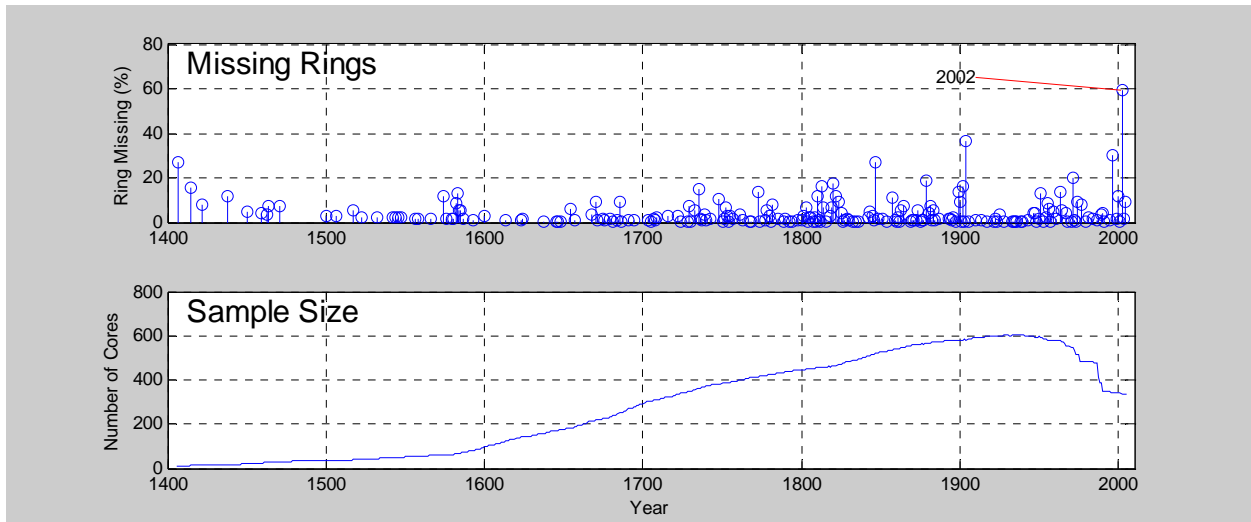

Figure 12. Missing ring percentage through time. The top panel shows the percentage of missing rings in each year (at all sites with available cores), and the bottom panel shows the number of available cores used to compute the percentage.

(3-c)   *Storage needs manifest themselves over several years. What does the reconstruction reveal about time-averaged flow during the current drought in the context of the past 6+ centuries?*

To examine this we plotted time-averaged reconstructed flows using a 6-year running mean (see **Figure 13**). We then identified those 6-year intervals when flow was equal to, or lower, than a baseline defined
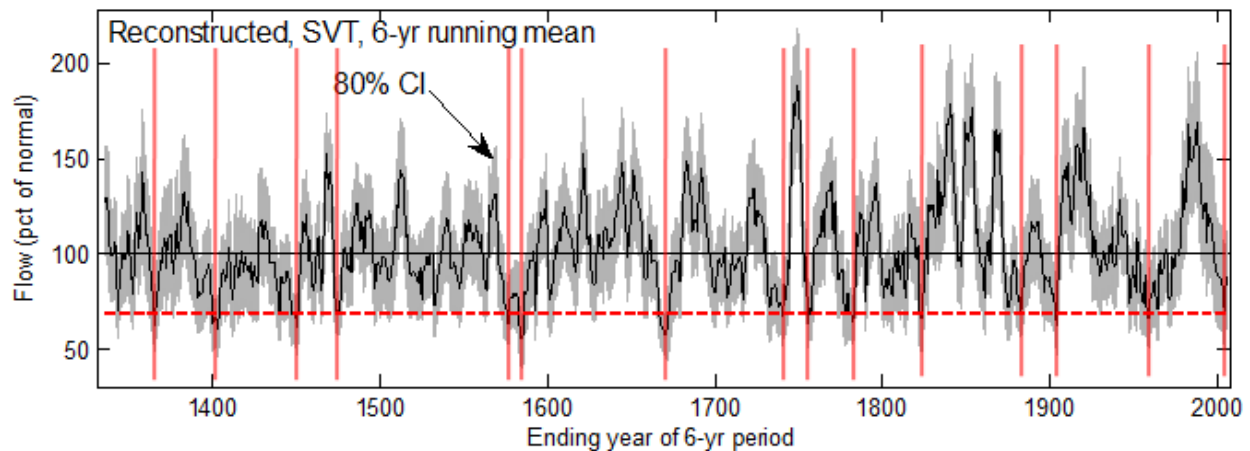
Figure 13. Variations in time-averaged flow, based on a 6-year running mean for 1330-2005. The solid black line represents averaged flows plotted as % of normal, where normal = the median of all 6-year running means. The gray areas define the 80% confidence interval for the reconstructed values. The reconstructed 6-year mean for the period 1999-2004 is plotted as a dashed red line to serve as a baseline comparison for the entire record. Vertical red lines indicate those 6-year intervals when flow was equal to, or lower, than the 1999-2004 baseline.

by the most severe 6-year period of the current drought: 1999-2004. There were 14 distinct prior occurrences of flow as low as 1999-2004 average (shown as vertical red bars in Figure 13.) The most severe conditions took place during the 6-year period ending at 1590 and again at 1670. The long-term record indicates that averaged low flow episodes as severe as the driest 6-year average during the current drought have occurred up to 3 times in each century since 1300.

(3-d)   *Wet years are extremely important during an extended drought period. How well can the reconstruction track the high flow years? What about extreme flood peaks?*

We investigated these questions via a case study of Verde River flows.[7] **Figure 14** is a graphical comparison of the time series of observed, reconstructed, and instantaneous peak flows for the Verde. Overall, tree ring reconstructions that rely on log-transformed flow data tend to do a better job capturing low flow extremes than high flow extremes. Figure 14 shows excellent correspondence between observed and reconstructed annual flow values in low flow years, and a reasonably strong agreement in high flow
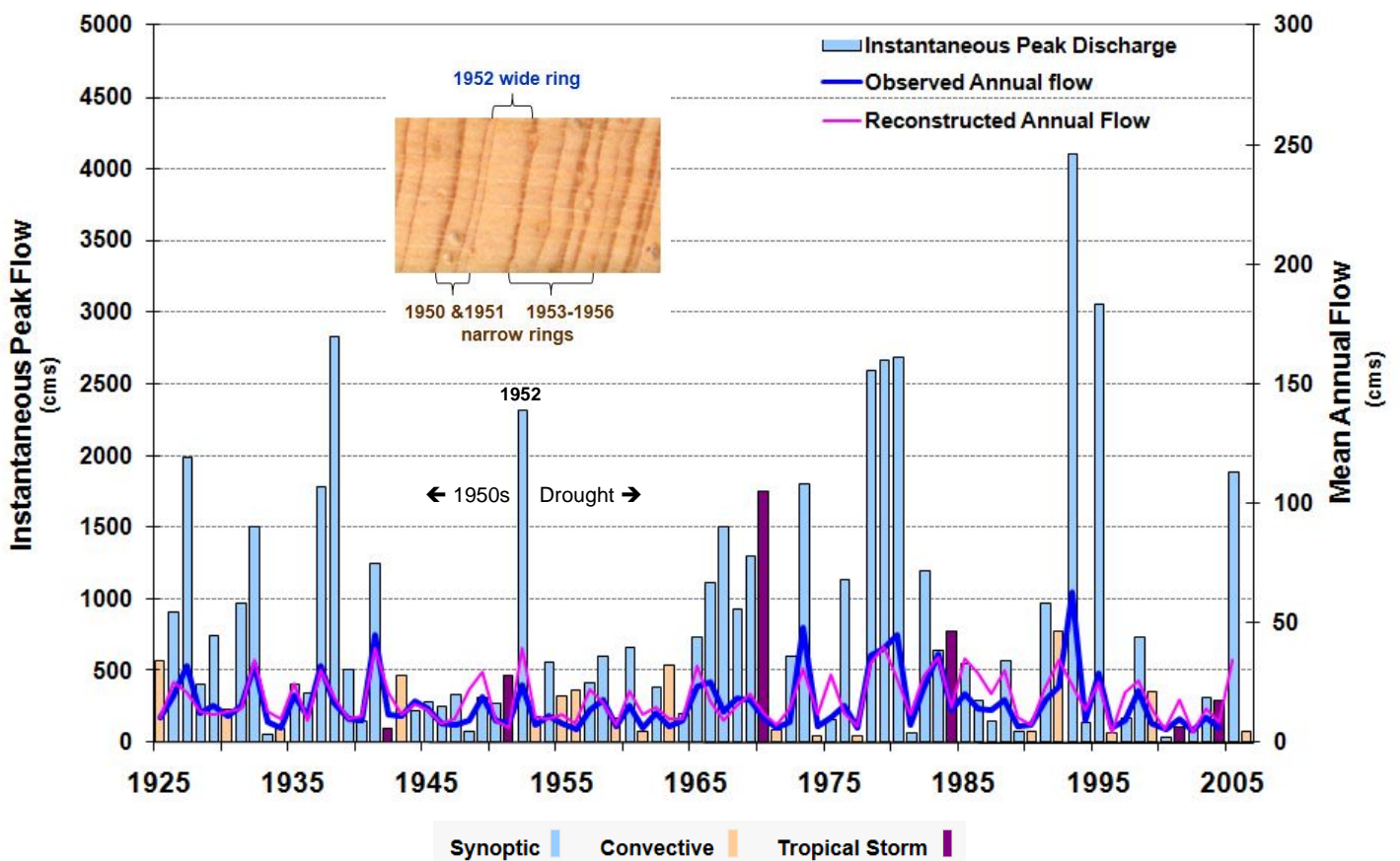

Figure 14. Verde River Basin Comparison of Observed, Reconstructed, & Instantaneous Peak Flows. Plotted for each year are the observed mean annual flow (dark blue line) and the tree-ring reconstructed mean annual flow (magenta line) in cubic meters per second (cms) for the Verde River[7] (scaled on the right axis). Also plotted is the instantaneous annual peak flow (vertical bars) in cms, (scaled on the left axis). The instantaneous peaks are classified and color coded to show the hydroclimatic cause of each event. The tree-ring core inset depicts a wide ring occurring within an otherwise narrow-ring sequence during the 1950s drought.

---

[7] Observed mean annual flow values were compiled from daily streamflow records of the Verde River below Bartlett Dam (USGS # 09510000) and, beginning in September 1945, from the Verde River below Tangle Creek, above Horseshoe Dam (USGS #09508500). The peak flow values are from the Verde River below Tangle Creek, above Horseshoe Dam. See Appendix 1.

years, including the capture of high annual values for most (but not all) years with exceptionally large instantaneous annual peak flows. **The ability of the reconstruction to track both low and high flows in the observed record lends confidence to the use of the streamflow reconstruction to identify drought-relieving high flow years in both the observed and reconstructed records.** The tree-ring core inset in Figure 14 shows an example of a very wide ring occurring in the middle of the extended 1950s drought period. The wide ring corresponds to the drought-relieving wet year of 1952 which is also captured in the reconstructed flow. The magnitude of the reconstructed value for 1952 may also be an indicator of the large annual flood peak (2,311 cms) that occurred on December 31, 1951. **Flood peaks produced by synoptic-scale winter storms tend to be better reflected in reconstructed streamflows than floods produced by summer convective or tropical-storm related flood events.** [8]

(3-e)   *What does the reconstruction reveal about the length of intervals between drought-relieving wet years in the long-term record?*

For drought planning, our Salt River Project collaborators wanted to know what the long-term record indicates about high flows as well as low flows—especially with respect to the typical length of time interval (or "gap") between drought-relieving high flows. Based on the positive results from our Verde case study on the ability of the reconstruction to track high flows as well as low flows, we concluded that this question could be addressed using the long-term record of reconstructed flows. For comparison, we first examined the gaps between wet years in the observed record (**Figure 15**.) We defined wet years as those above a threshold of the 75th percentile of observed annual flow (> 1504 kaf). Based on this criterion, 23 of the 94 years in the record were classified as wet (indicated by circles in Figure 15.) We then computed the interval, or gap, as the number of consecutive years between successive designated wet years. (This interval was 0 if wet years were adjacent). Results indicated **that the median interval between wet years in the observed record is only 2 years. The widest wet-year gap of the observed record was 13 years and occurred during the 1950s drought** (pink shading). If not for the wet year of 1952 (see Figure 14), this interval would have been 25 years. **The wet-year gap during the current drought was 9 years** (gold shading).
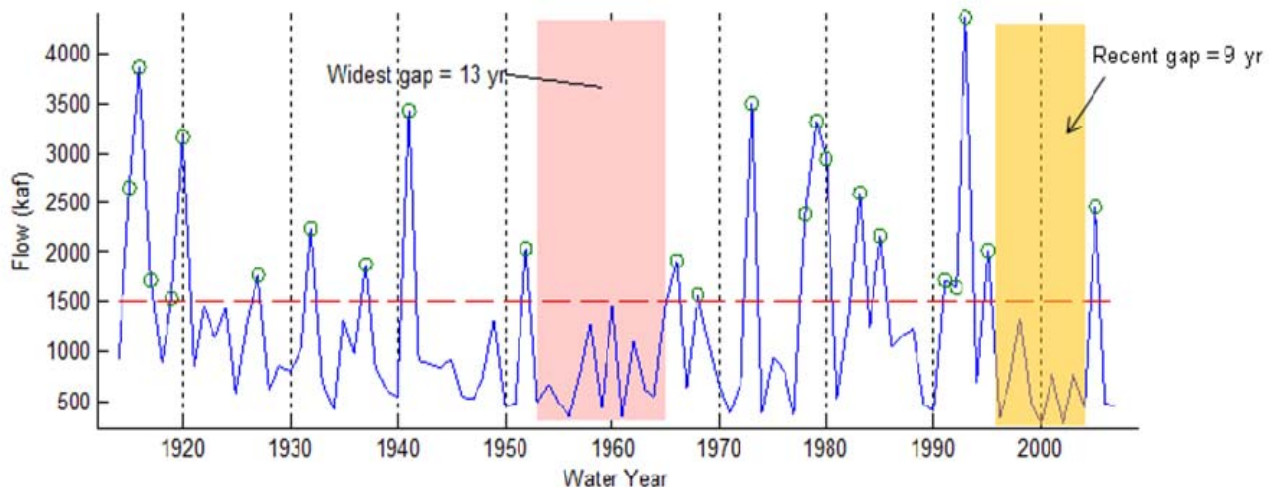

Figure 15. Length of intervals between wet years for the Salt + Verde + Tonto based on observed flows, 1914-2007. Values are mean annual in thousands of acre feet (kaf). "Wet Years" are identified with circles and are defined as years having an annual flow > the 75th percentile = 1504 kaf (dashed red line).

---

[8] A notable exception is the record-breaking winter flooding year of 1993, which was not captured well by the reconstruction. One explanation for this is that the soil was so saturated during this event that large amounts of excess runoff were unusable by the trees and did not affect their growth.

We then performed the same analysis on the 676-year S+V+T reconstructed flow record (**Figure 16)** and compared the results in the observed and reconstructed records (**Figure 17**). We found that, **in the reconstructed low flows, the median interval between wet years was 3 years, and the longest interval was 22 years** (1382-1403). Other large intervals were the 20-yr gap ending in 1585 and the two 16-yr gaps ending in 1676 and 1742. Note that the reconstruction for the S+V+T does not perfectly classify the wet years of the observed record. (For example, 1993 was a wet year in the observed, but not in the tree-ring record.) This is why **the "recent gap" associated with the current drought is 12 years long** when derived from reconstructed flows (**Figure 16**), compared to the shorter 9-year gap derived from observed flows (Figure 15). Another 12-year interval took place in conjunction with the 1950s drought (1953-1964). **Overall in the reconstructed flows, there were 10 intervals between wet years that were greater than, or equal to, 12 years. This suggests that the persistence of the current drought—unrelieved by an intervening high flow for up to 12 years— is by no means unique in the context of the long-term record.**
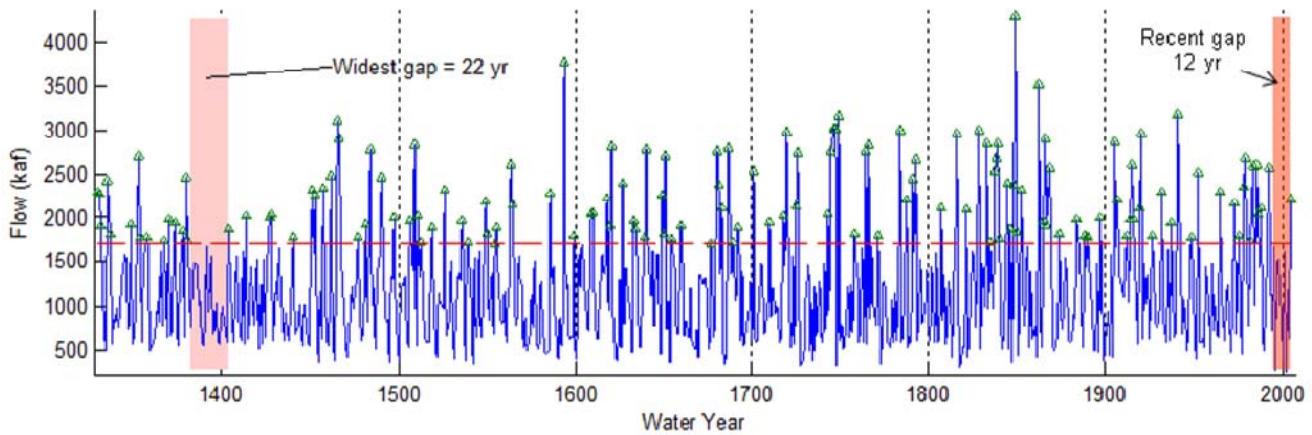

Figure 16. Length of intervals between wet years for the Salt + Verde + Tonto based on reconstructed flows, 1330-2005. Wet years defined as in Figure 15, but for the reconstructed flow, and identified by triangles. The horizontal red line represents the 75th percentile threshold for classifying wet years in the long-term record. Red shading highlights two of the intervals noted in the text.
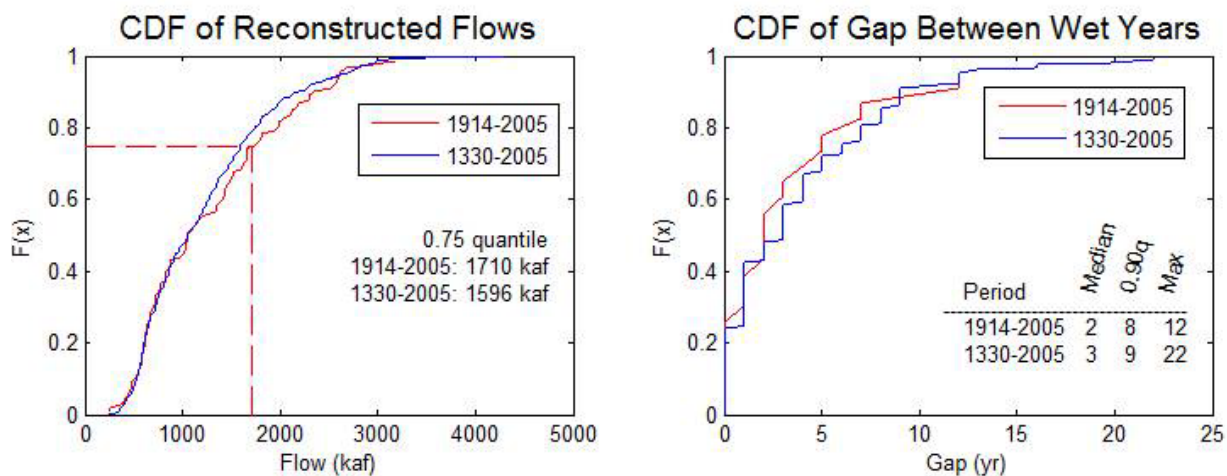

Figure 17. Comparison of the length of intervals between wet years in the instrumental and long-term records. (a) Cumulative distribution functions (cdfs) of the reconstructed flows for the entire reconstruction (blue line) and for the period of the reconstruction that overlaps observed flows (red line), (b) Cumulative distribution functions of the gap, or interval, between wet years, again for both the full-length reconstruction (blue) and the part that overlaps observed flows (red).

- 18 -

Figure 17 compares wet-year gaps in the observed (instrumental) and reconstructed records. **Figure 17a** shows the cumulative distribution functions (cdfs) of reconstructed flows for the entire period of record (blue line) and for the period of the reconstruction that overlaps with the observed flow record (red line). This depiction of the results reveals that the 0.75 quantile (used for classifying the wet years) is slightly lower for the 1330-2005 than for 1914-2005. The difference is a bit over 100,000 acre-ft. **This is consistent with general observation that the long-term record is a bit drier than the instrumental period.**

Figure 17b summarizes the time, or gap, between wet years. It shows the cumulative distribution functions (cdfs) of the time interval (gap), between wet years, for the entire period of record (blue line) and for the period of the reconstruction that overlaps with the observed flow record (red line). If two consecutive years are above the 0.75 quantile, the "gap" is defined as zero. **The median gap for both the long-term and the observed period is 3 years.** The 0.90 quantiles are also equal, at 9 years. The difference emerges in the extremes. The 1330-2005 record contains a 22-year gap, around the start of the 15th century. In contrast, the longest gap in the more recent 1913-2005 part of the reconstruction is 12 years (1953-1964 and 1993-2004). This depiction of the data echoes the discussion for Figure 16 above and confirms that **the persistence of the current drought is not unprecedented, and at least one drought occurred in the past that was nearly twice as long as the current drought.**

(3-f)   *Can seasonal information about the relative contribution of winter vs. summer flows be deciphered in the tree-ring reconstruction?*

Previous work in Arizona suggested that latewood widths may carry a signal of summer precipitation (Meko and Baisan 2001). We explored this question further by relating partial ring measurements of latewood at a few sites to monthly precipitation data using an input-output model (**Figure 18**.) The model results
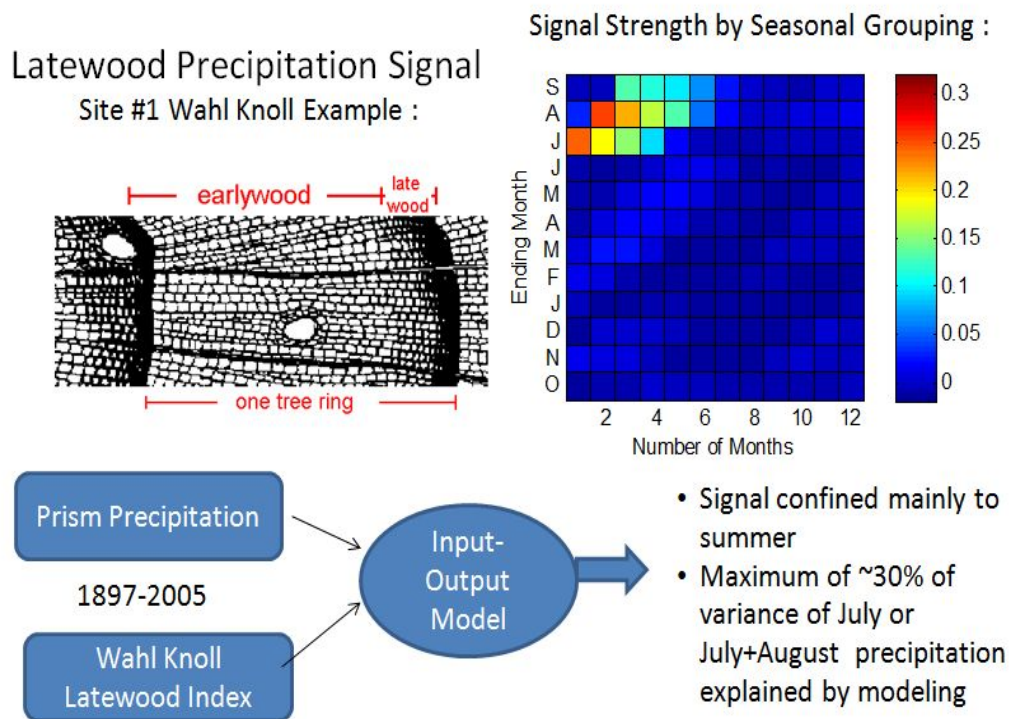

Figure 18. Example of exploration of latewood signal strength at a single site using a precipitation input/latewood output model. The dark red square on the signal-strength graph indicates that the strongest correlation between latewood width and precipitation occurred during the 2-month period ending in August.

showed that latewood width had a weak but significant signal for summer precipitation. However, the importance of this weak partial-ring signal for summer does not appear to be reflected in the total ring width which had a strong signal for annual precipitation, but not for summer precipitation. While these results were encouraging, we concluded that the summer precipitation signal in partial ring widths is too weak to expect useful reconstruction of summer monsoon variability from this limited site coverage.[9]

4 –CLIMATIC CONTEXT AND DISCUSSION

 (4-a)   *Based on these analyses, what is the prediction for how long the current drought will last and what is the forecast for future drought variability in the SVT due to climate change?*

As dendrochronologists, we use the present to reconstruct and interpret the past. Our analyses cannot provide either short-term predictions or long-term forecasts about water supply, nor do we incorporate models of future climate change into our interpretation of our results (although this may become a fruitful area of research in the future). Rather, **the value of a tree-ring reconstruction of streamflow lies in its lengthy record of events that have already occurred) and the resulting statistics such a record yields.** Both the increasing demand for water due to population growth and climate model projections of future drier conditions in the Southwest (e.g., Seager et al, 2007) are sure to exacerbate future drought conditions in the SVT. Our tree-ring reconstructions can provide the probabilistic baseline upon which to evaluate future changes in magnitude and frequencies of these extremes. If, as some have speculated, the current drought is a manifestation of climate change already at work, **our evaluation of the drought in the context of the long-term record illustrates its uniqueness (at least in terms of single-year extremes).** We cannot say whether this is a harbinger of the future.

 (4-b)   *What is the global and regional climatic context in which the current SVT drought has evolved? Does it relate to global warming?*

Our previous study (LTRR-SRP-I) examined the regional context of synchronous extreme streamflow episodes in the Salt-Verde-Tonto and Upper Colorado River basins and found a strong tendency for the joint occurrence of extreme flow years (low and high) in both basins. The time series of observed flow for the two basins in shown in **Figure 19**, along with the time series of average Northern Hemisphere temperatures since 1880, the so-called global warming curve. Figure 19 illustrates the severity of the
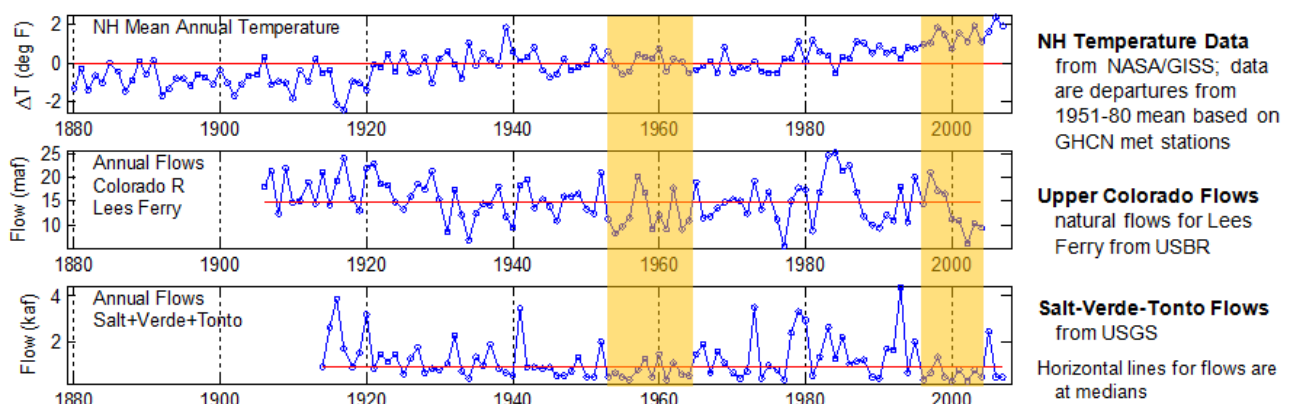

Figure 19. The global and regional climate context. Shown are instrumental record time series of : *(top)* Northern Hemisphere mean annual temperature data (source: http://data.giss.nasa.gov/gistemp/), *(middle)* annual streamflow for the Colorado River at Lees Ferry, and *(bottom)* S+V+T observed annual flows. The orange shading brackets the time intervals of the 1950s and current drought in the S+V+T for comparison with the other two time series.

---

[9] For more details on the latewood measurements and summer signal analysis, contact the authors.

current drought in both the SVT and Colorado basins in the late 1990s and early 2000s, a period when the average Northern Hemisphere temperature was well above normal (where normal is defined as the 1951-1980 mean). However, the 1950s drought, which also occurred in both basins and was exceptionally dry in the SVT, took place during a period of normal Northern Hemisphere temperatures, and the dry years of the early 1900s in the Colorado and SVT (not shown) took place during a period of below-normal Northern Hemisphere temperatures. **This illustration highlights the futility of trying to draw a <u>simple</u> cause-and-effect relationship between the severity of the current drought and climate change or global warming, as manifested in the time series of a hemispheric temperature curve.** Rather, better questions to ask are: *(1) What regional atmospheric circulation patterns are associated with extreme low flow years and high flow years in the SVT streamflow record, and (2) Are there any factors related to global climate that would cause a change in the magnitude, frequency, or location of these patterns?*

(4-c)   *What regional atmospheric circulation patterns are associated with extreme low flow years and high flow years in the SVT streamflow record?*

The updated streamflow reconstruction for the Salt + Tonto + Verde basin provides exceptional information about the range of variability of low and high flow extremes in this basin over the past 6+ centuries. Determining the likely climatic causes of these past extreme episodes is more difficult. Our approach is to gain an understanding of how the observed and reconstructed flows vary in response to climatic drivers and atmospheric circulation patterns during the instrumental record, and then use this knowledge to infer the most likely causes for past extreme streamflow episodes.

As noted above, the LTRR-SRP-I project addressed the joint occurrence of low flow years and high flow years in both the SVT and Upper Colorado River (UCRB) basins. We found that distinctly different— and inverse— atmospheric circulation patterns were dominant during joint low flow vs. high flow years. **Figure 20** shows these contrasting patterns, updated with additional low-flow years from the current drought. The figure indicates that anomalously high 700 mb geopotential heights (upper-level ridges) dominated the North Pacific Ocean and western United States, extending over a broad latitudinal band in winter during extreme regional drought years in both the SVT and UCRB. The high flow years in both basins were linked to anomalously low 700 mb heights (upper level troughs) concentrated in the eastern North Pacific and the far western states, also over a broad latitudinal band. In our earlier study we had noted an apparent shift in the position of seasonal anomaly centers in the composites of the joint high flow (HH) and low flow (LL) years. We had observed that (in LL years especially) a positive (high)
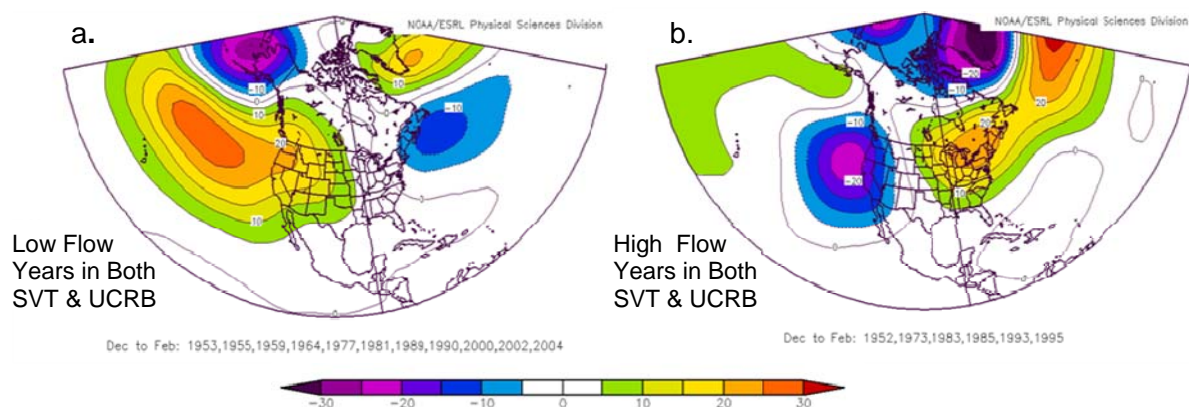

Figure 20. Winter atmospheric circulation patterns during years with joint occurrence of (a) low flow and (b) high flow in both the Salt-Verde-Tonto (SVT) and Upper Colorado River Basin (UCRB). The figures depict composite anomaly charts of the Dec – Feb 700 millibar (mb) geopotential heights for those years in which exceptional annual low flow or high flow predominated in both basins. Anomaly values are in meters and are based on the period 1968-1996. Red/orange = strong positive height anomaly or dominance of upper level high pressure; purple/blue = strong negative height anomaly or dominance of upper level low pressure.

seasonal pressure height anomaly was situated over the western continental U.S. during the early half of the cool season (Oct-Dec), but shifted to the eastern North Pacific Ocean during the second half of the cool season (Jan-Mar). To see if this seasonal shift was evident in the SVT, we constructed early- and late-season winter composite anomaly maps for six SVT low-flow years of the 1950s drought (**Figure 21**) and the current drought (**Figure 22**). We also constructed maps for each year to see how representative the 6-year seasonal composites were of individual year variability. The left hand panel in each figure depicts anomaly maps for three different seasonal groupings: (a) the core winter (Dec-Jan-Feb), (b) the early cool season (Oct- Nov-Dec) and (c) the late cool season (Jan-Feb-Mar). The right hand panel shows early- and late-winter circulation patterns for each of the individual years.

The resulting patterns **underscore the importance of separating the winter/cool season into early and late portions when assessing climatic anomalies.** The early→ late westward shift of the positive pressure anomaly can be seen in the 6-year composites of both the 1950s and current droughts, as well as in most of the individual years. A correlation map analysis (not shown) indicated that both early- and late-winter circulation patterns influence annual flow variability in the SVT but in different ways— a result which echoes the seasonal anomaly patterns in Figures 21 and 22. **These results indicate a strong similarity between the 1950s and current drought in their associated large-scale circulation patterns**. However, the positive height anomalies over the continent in OND, and ocean in JFM, were
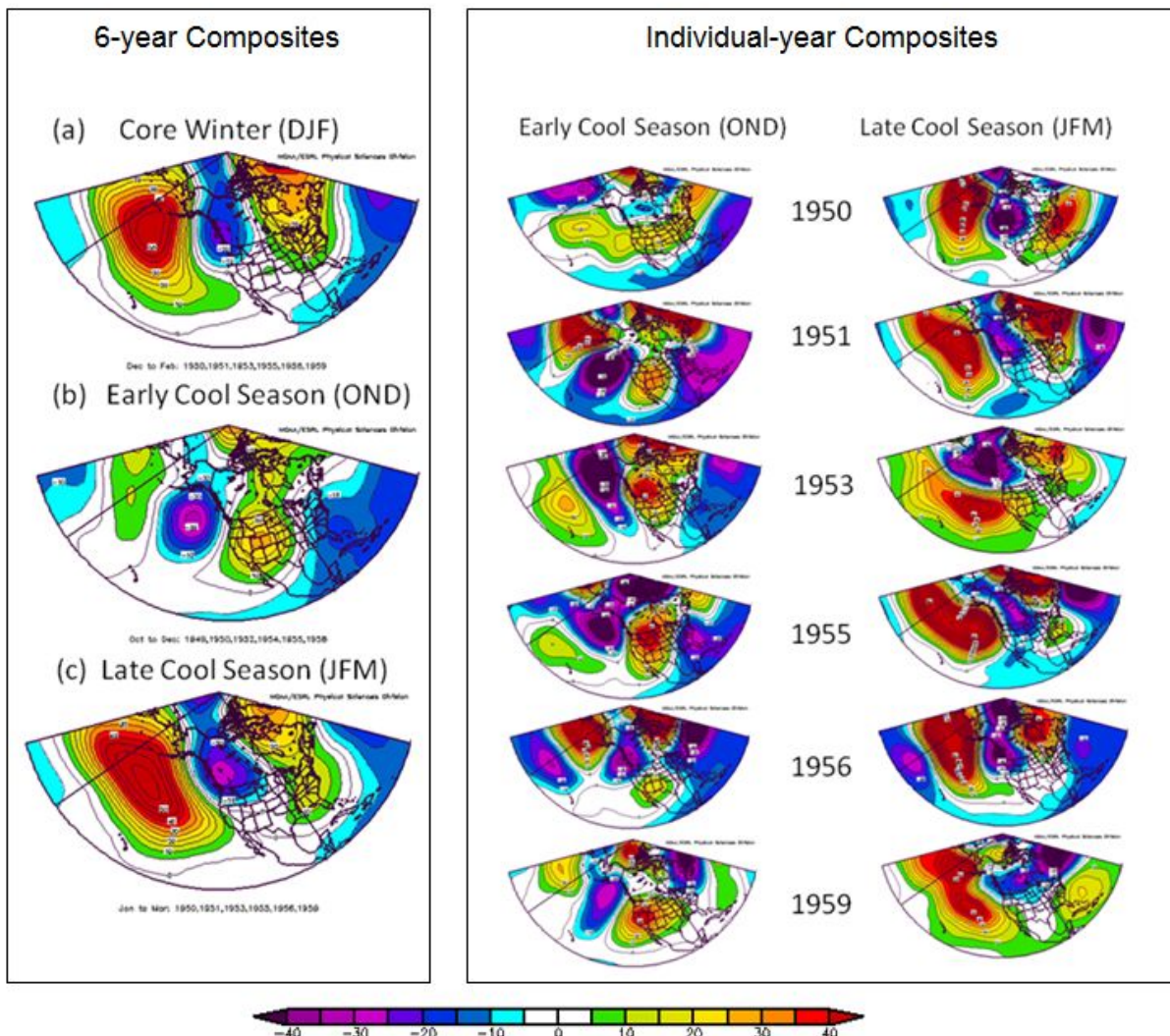

Figure 21. Seasonal circulation anomaly patterns for 6 low flow years during the 1950s drought in the Salt+Verde+Tonto. Maps are composite anomalies as in Figure 20. (a), (b) and (c) in the left panel
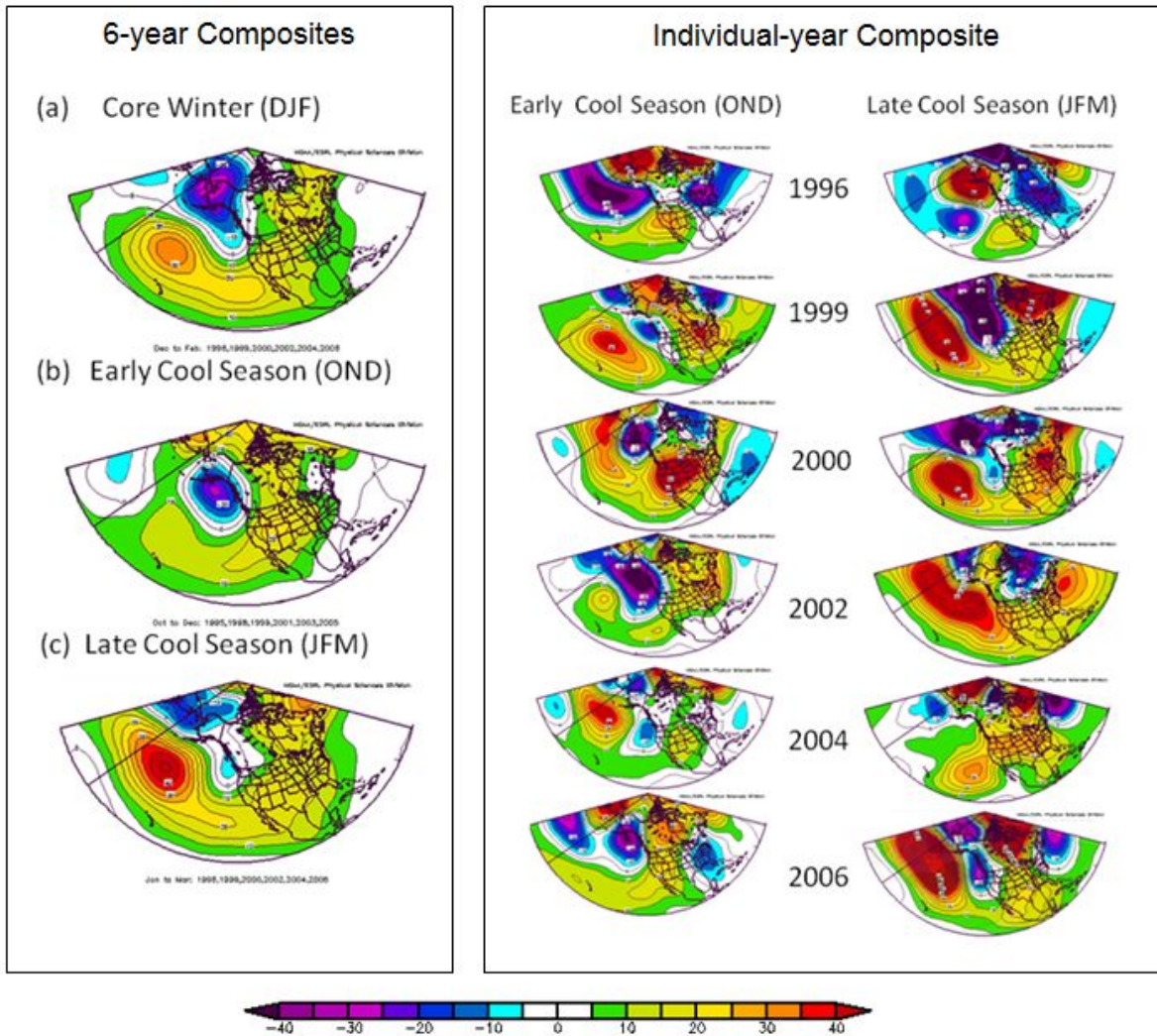
CURRENT DROUGHT – LOW FLOW YEARS

Figure 22. Seasonal circulation anomaly patterns for 6 low flow years during the current drought in the Salt+Verde+Tonto. Same as Figure 21, but for low-flow years during the current drought.

stronger during the 1950s drought overall, and in most individual years— which explains why its severity and persistence exceeded that of the current drought, except in 2002.

Figure 20 suggests that high flow years are associated with a circulation pattern that is inverse to that of the low flow years. We found this same result in the SVT when we mapped the anomaly patterns for 1952 (an important drought-relieving year during the 1950s with a wide tree ring, see Figure 14), and 2005 (a relatively wet year with a moderately wide tree ring during the current drought) (**Figure 23**). The negative (low pressure) anomalies were stronger in 1952 than 2005 in both early and late winter.

The strength of the positive and negative circulation anomalies during the extreme flow years in the SVT is indicative of one or more of several factors: the persistence (or repeated development) of a ridge or trough pattern in the same general location, the intensity of upper-level high or low pressures, and/or the unusual or unseasonal location of the circulation features. We observed that *atmospheric blocking,* [10] or

---

[10] "The obstructing, on a large scale, of the normal west-to-east progress of migratory cyclones and anticyclones." (AMS *Glossary of Meteorology*). More specifically, it " involves the formation of quasi-stationary, long-lived 7-days), closed anticyclonic circulation cells that temporarily divert the prevailing west-to-east flow of air at middle and upper tropospheric levels.." (Thompson & Wallace 2001, p. 85)

**Early & Late Cool Season Patterns
for Two Drought-Relieving High Flow Years**

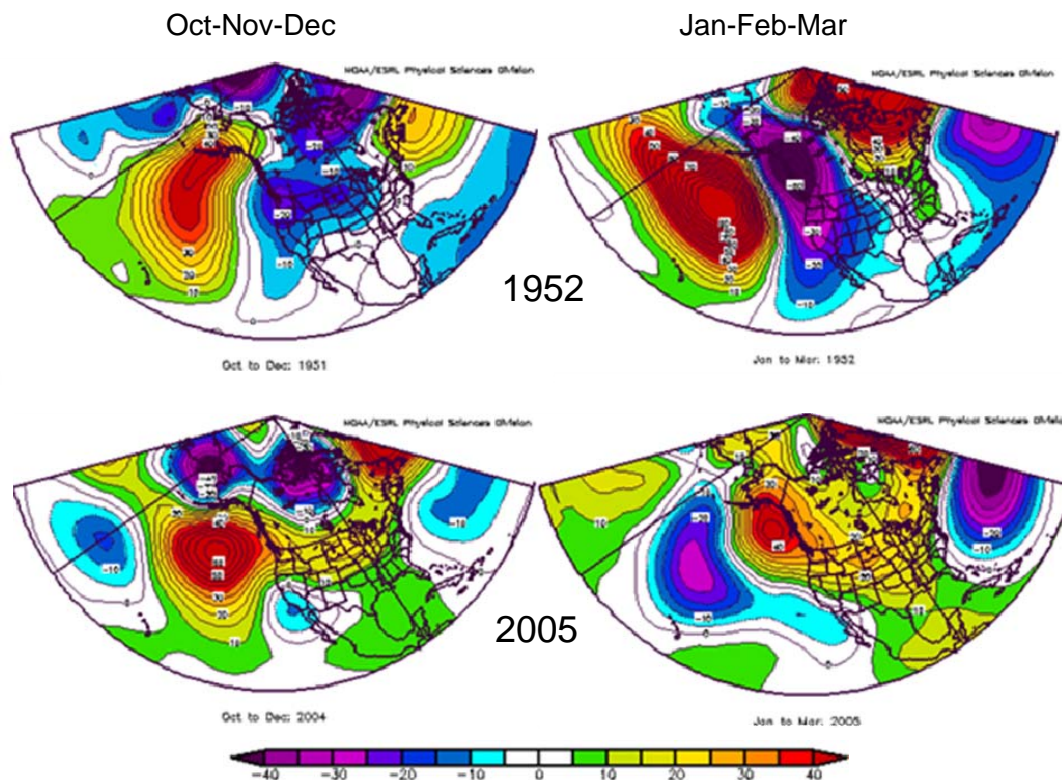Oct-Nov-Dec   Jan-Feb-Mar

**Figure 23. Seasonal circulation patterns for two drought-relieving years occurring
during the 1950s and current drought.** Maps are composite anomalies as in Figure 20.

blocking-like behavior—along with its associated upper level upstream and downstream troughs—played
a role in several of the synoptic circulation patterns for individual winter months during the extreme low
and high flow years in the SVT.[11] **Figure 24** presents two examples of episodes with persistent blocking-
like, high amplitude trough-ridge-trough patterns that affected the flow in the SVT. As Figure 23
illustrates, blocking-like patterns can be linked to both droughts and floods, depending on the longitudinal
positioning of the trough-ridge-trough pattern with respect to a watershed **Because of their persistence,
we expect that blocking-related circulation patterns are likely to be reflected in unusually wide or
narrow tree ring widths.** We hope to explore this connection in more detail during future research,
especially in the context of recent literature that has identified associations between North Pacific
blocking patterns, early and late-winter dynamical trends in the Northern Hemisphere, trends in some
climate indices, and a possible link to greenhouse gas forcing (Thompson and Wallace 2001, Fei et al.
2002, Carrera et al. 2004, Hu et al. 2005)

Figure 25 summarizes the discussion above by annotating the Verde River time series of observed,
reconstructed and peak flows with examples of some of the key circulation anomaly patterns associated
with low, high, and peak flows in the basin to answer the question: *What regional atmospheric
circulation patterns are associated with extreme low flow years and high flow years in the SVT
streamflow record?* We propose that these same patterns can be applied to the long-term record of
reconstructed SVT flows to explain how the extremes of the past may have occurred.

---

[11] Namias made this same observation with respect to the Far Western drought of winter 1977, an extreme low flow
year in the SVT: " . . the isobaric signature of drought suggest anticyclonic vorticity associated with high pressure
ridges, or at times, high pressure cells. These ridges serve as blocks to cyclonic activity from the Pacific, and often
displace storm tracks north of the United States/Canadian border. . . . the anticyclonic ridge may often be responsive
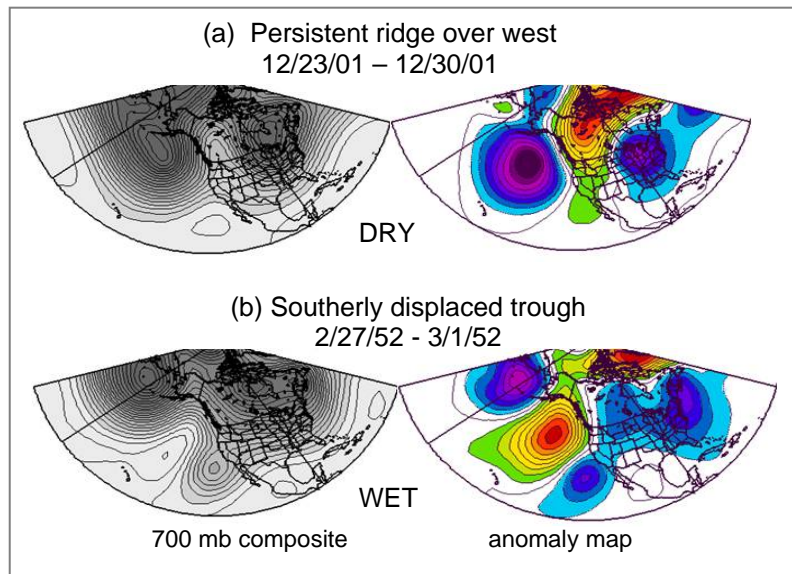to an upstream trough over the eastern United States." Namias 1983, p 35).

Figure 24. Examples of episodes with persistent blocking-like, high amplitude trough-ridge-trough patterns. (a) depicts an 8-day composite and anomaly map for a blocking-like episode in December 2001 that exacerbated the extremely dry conditions of water year 2002. (b) depicts a 4-day composite and anomaly map for a blocking-like episode that displaced the Pacific storm track unusually far south, leading to one of several drought-relieving wet episodes during 1952.
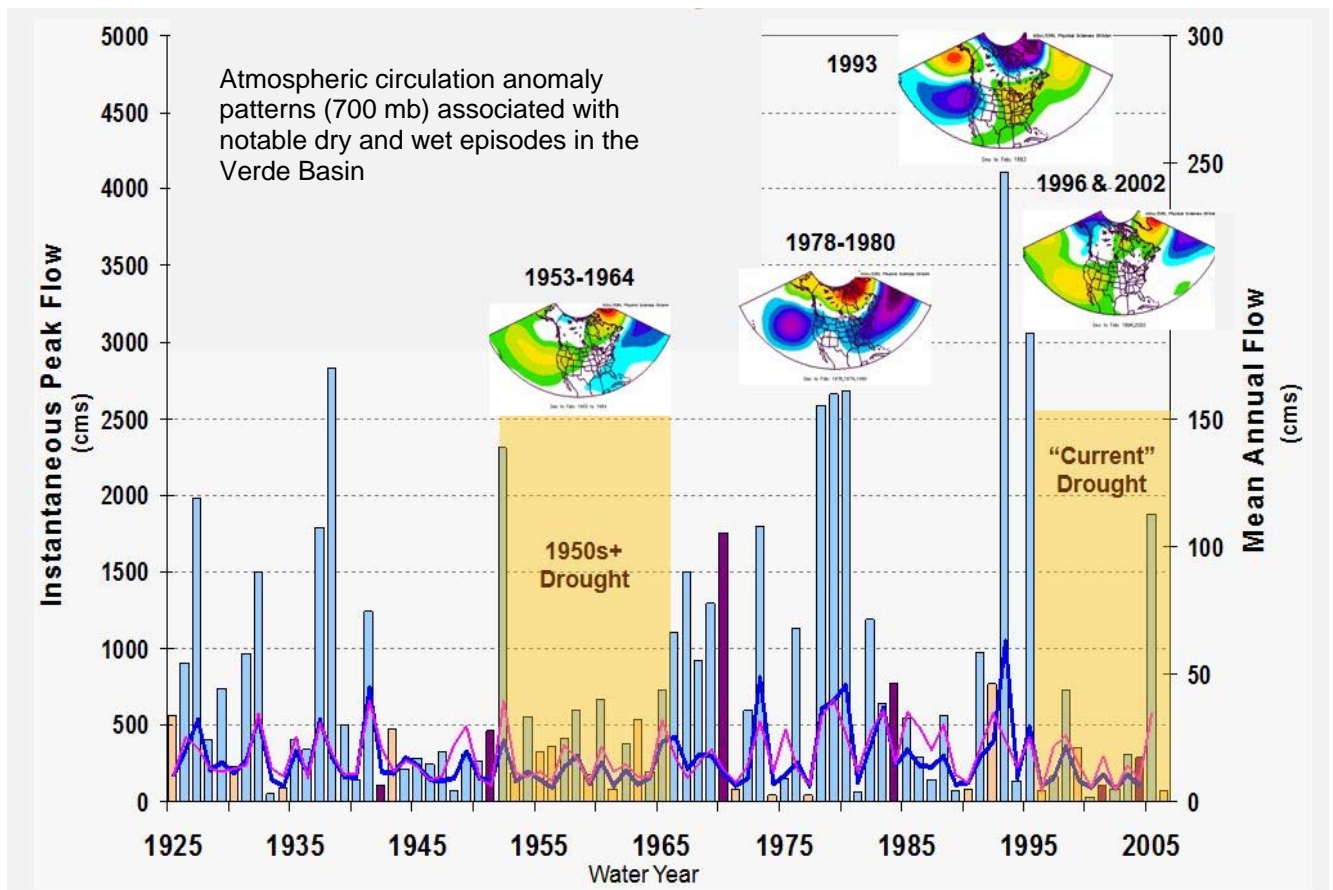

Figure 25. Atmospheric circulation anomaly patterns (700 mb) associated with notable dry and wet episodes in the Verde Basin. Observed, reconstructed, and peak flow as in Figure 14. The inset circulation patterns are examples of representative composite anomaly patterns for the different episodes.

(4-d)   *Are there any factors related to global climate that would cause a change in the magnitude, frequency, or location of the regional circulation patterns associated with low and high flows?*

As noted above, recent literature has suggested some possible linkages between hemispheric-wide atmospheric dynamics, circulation indices, and regional climate extremes, such as those related to blocking-like patterns. A detailed inspection of these proposed linkages in the context of the current drought was beyond the scope of this project. We did, however, explore the relationship between a few circulation/sea surface temperature indices and SVT low and high flow years (**Figure 26**). As in the LTRR-SRP-I study, **low flow years were more frequent in association with +AMO and – PDO, but not limited to this association**. La Niña years (as defined by + SOI) were more likely to be associated with low flow than high flow, but some low flow years also occurred in association with –SOI and a weak El Niño. In contrast, **high flows did not occur in association with any moderate or strong La Niña years, instead they were associated with either a neutral or strongly negative SOI. High flow years were also more frequent in association with +PNA** (which is in keeping with the tendency for the positive phase of the PNA to be associated with El Niño).   These results agree with similar findings for the same indices and Arizona precipitation variability.
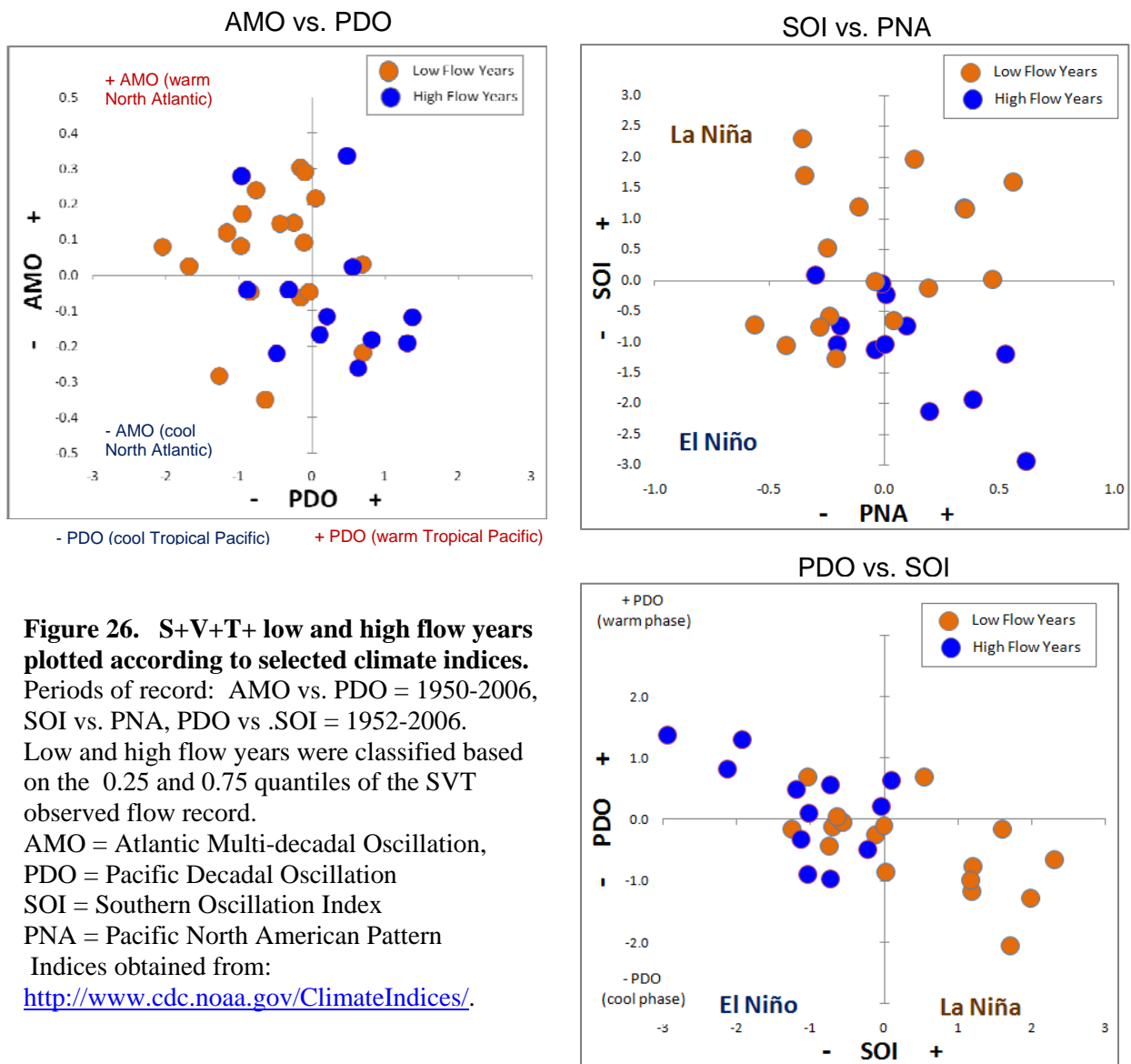

Figure 26.   S+V+T+ low and high flow years plotted according to selected climate indices. Periods of record: AMO vs. PDO = 1950-2006, SOI vs. PNA, PDO vs .SOI = 1952-2006. Low and high flow years were classified based on the 0.25 and 0.75 quantiles of the SVT observed flow record. AMO = Atlantic Multi-decadal Oscillation, PDO = Pacific Decadal Oscillation SOI = Southern Oscillation Index PNA = Pacific North American Pattern Indices obtained from: http://www.cdc.noaa.gov/ClimateIndices/.

The utility of the index-based method for differentiating between low and high flow years in the SVT watershed may be hindered by the generalized geographic range of synoptic patterns that can be associated with different index phases. This reinforces the importance of a companion approach that focuses on the synoptic circulation patterns specifically linked to low and high flows in a given watershed (as described in section 4-c). Such an approach can also identify the weather and climate patterns that lead to wide and narrow tree rings, thereby providing a mechanistic basis for the causes of the variations and extremes seen in both streamflow and ring widths.

The question posed at the beginning of this section — *Are there any factors related to global climate that would cause a change in the magnitude, frequency, or location of the regional circulation patterns associated with low and high flows?* — remains the central question for determining whether the severity of the current drought is a manifestation of climate change and/ or global warming. Further research is needed on several fronts to determine the answer.

5 – SUMMARY AND CONCLUSIONS

This project updated the tree-ring reconstructions of annual streamflow of the Salt-Verde-Tonto Basin (SVT) through the period of the current (and ongoing) drought of the late-1990s and early 2000's using new tree-ring data collected in 2005. Ring widths of the new collections were found to have a strong annual runoff signal. The newly collected data were combined with existing collections of varying record length to produce a new reconstruction by blending together three subset models. The updated SVT reconstruction covers the period 1330-2005 and explains 49- 69% of the variance of the annual flows.

The main goal of the project was to re-calibrate, update, and analyze the SVT tree-ring reconstructions of streamflow using the new collections and chronologies in order to place the most recent drought and high flow extreme years in the context of the entire record, including present and past climatic variability.

Following is a summary of our major findings:

1) Overall, the reconstruction of annual streamflow indicates that the long-term record has been slightly drier than the instrumental record.
   .
2) With respect to single-year low flow extremes in the new reconstruction, recent years of the current drought (1996 and 2002) were unsurpassed in the long-term tree-ring record of flow.

   - The reconstructed 2002 value was the lowest reconstructed flow, and the reconstructed 1996 value was the 2nd lowest reconstructed flow, since 1330.

   - From the perspective of growth stress on the trees cored for the new collections, the year 2002 was unprecedented: 60% of 300+ cores were missing the 2002 ring.

3) With respect to multi-year (6-year) low flow extremes, the current drought is *not* the most extreme in the long-term record. The reconstruction indicates that there were 14 distinct prior occurrences of 6-year flow as low as the 1999-2004 average, including periods in the early 1900s and 1950s. Using the observed 1814-2006 median flow as "normal," 28 other periods were more continuously severe than the current drought in terms of "consecutive years below normal."

4) When viewed from the perspective of the length of time between "drought relieving" wet years in the reconstructed low flows, the median interval between wet years was 3 years, and the longest interval was 22 years (1382-1403). In contrast, the longest gap in the more recent 1913-2005 record was 12 years and occurred twice: 1953-1964 and 1993-2004.

5) Circulation anomaly patterns associated with winter storm track positions reveal a signature drought pattern. There is a strong similarity between the 1950s and current drought's circulation, with a shift occurring from early- to late-winter. Anomalies were stronger during the 1950s.

- Circulation anomaly patterns associated with extreme high flows were the inverse of those associated with low flows and were similar to patterns identified for extreme years occurring jointly in the SVT and Upper Colorado River Basins (as defined in the LTRR-SRP-I project).

- Blocking-like behavior played a role in several of the synoptic circulation patterns for individual winter months during the extreme low and high flow years.

- Climate indices have some ability to differentiate between low and high flow years, but a definitive link to the ultimate drivers of global climate change requires more research.

The overall conclusion to draw from these findings is that current drought is by no means unique in the context of the long-term record. Despite the unprecedented single-year severity of 1996 and 2002— the multi-year persistence of the current drought (as of 2006) has not been unprecedented. At least one drought occurred in the past that was nearly twice as long as the current drought and 28 other droughts were more continuously severe in terms of "consecutive years below normal" in the long-term record.

The following appendices are available at: http://fp.arizona.edu/kkh/srp2.htm

APPENDIX 1 - Listing Of Observed Water-Year Average Flows
APPENDIX 2- Field Collections and Ring-Width Data
APPENDIX 3 - Chronology Development
APPENDIX 4 - Reconstruction Method
APPENDIX 5 - Tree-Ring Reconstruction of Streamflow by Scatterplot Smoothing (manuscript)

REFERENCES

Carrera, M.L., R.W. Higgins, and V.E. Kousky (2004) Downstream Weather Impacts Associated with Atmospheric Blocking over the Northeast Pacific. *J. Climate*, 17, 4823–4839.

Cook, E.R., and Kairiukstis, L.A., editors (1990) *Methods of dendrochronology: applications in the environmental sciences*: Boston, Kluwer Academic Publishers, 394 p.

Cook and Peters, K. (1981) The smoothing spline: A new approach to standardizing forest interior tree-ring width series for dendroclimatic studies. *Tree-Ring Bulletin* 41, 45-53.

Cook, E.R., Meko, D.M., Stahle, D.W., and Cleaveland, M.K. (1999) Drought reconstructions for the continental United States. *J. of Climate*, v. 12, p. 1145-1162.

Cook, E.R., Woodhouse, C., Eakin, C.M., Meko, D.M., and Stahle, D.W. (2004) Long-term aridity changes in the western United States. *Science*, v. 306, p. 1015-1018.

Fei, Huang, Zhou Faxiu and Qian Xiaodan (2002) Interannual and decadal variability of the North Pacific blocking and its relationship to SST, teleconnection and storm tracks. *Advances in Atmospheric Sciences* **19**: 808-820.

Fritts, H.C. (1976) *Tree rings and climate*. London, Academic Press, 567 pp.

Gordon, G. (1982) Verification of dendroclimatic reconstructions, In: M.K. Hughes et al. (eds.), *Climate from tree rings*. Cambridge University Press, Cambridge, UK, 58-61.

Granger, C.W.J., and Hatanaka, M. (1964) *Spectral analysis of economic time series*. Princeton, New Jersey, Princeton University Press.

Graybill, D.A., Gregory, D.A., Funkhouser, G.S., and Nials, F.L. (2006) Long-term streamflow reconstructions, river channel morphology, and aboriginal irrigation systems along the Salt and Gila Rivers, In: *Environmental Change and Human Adaptation in the Ancient Southwest*, edited by Jeffrey S. Dean and David E. Doyel. University of Utah Press.

Hu, Y., K.K. Tung, and J. Liu (2005) A Closer Comparison of Early and Late-Winter Atmospheric Trends in the Northern Hemisphere. *J. Climate*, 18, 3204–3216.

LTRR-SRP-I (2005) *A Tree-Ring Based Assessment of Synchronous Extreme Streamflow Episodes in the Upper Colorado & Salt-Verde-Tonto River Basins* – Final Report. http://www.ltrr.arizona.edu/srp.htm

Meko, D.M. and Baisan, C.H. (2001) Pilot study of latewood-width of conifers as an indicator of variability of summer rainfall in the North American Monsoon region: *International Journal of Climatology*, 21:697-708.

Meko, D.M., and Graybill, D.A., 1995, Tree-ring reconstruction of Upper Gila River discharge: Water Resources Bulletin, v. 31, no. 4, p. 605-616.

Meko, D.M., Cook, E.R., Stahle, D.W., Stockton, C.W., and Hughes, M.K. (1993) Spatial patterns of tree-growth anomalies in the United States and southeastern Canada. *J. of Climate*, v. 6, p. 1773-1786.

Meko, D.M., Therrell, M.D., Baisan, C.H., and Hughes, M.K. (2001) Sacramento River flow reconstructed to A.D. 869 from tree rings. *J. of the American Water Resources Association*, v. 37, no. 4, p. 1029-1040.

Namias, J. (1983) Some causes of United States drought. *Journal of Climate and Applied Meteorology*, 22,30-39.

Seager et al., (2007) Model projections of an imminent transition to a more arid climate in Southwestern North America. *Science* 316 (5828), 1181. [DOI: 10.1126/science.1139601]

Smith, L.P., and Stockton, C.W. (1981) Reconstructed streamflow for the Salt and Verde Rivers from tree-ring data. *Water Resources Bulletin*, v. 17, no. 6, p. 939-947.

Stahle, D.W. and others (2000) Tree-ring data document 16th century megadrought over North America. *EOS Transactions*, v. 81, no. 12, p. 121-125.

Stockton, C.W. (1975) *Long term streamflow records reconstructed from tree rings*, University of Arizona Press, Tucson, Arizona, 111 pp.

Stockton, C.W., and Jacoby, G.C. (1976) *Long-term surface-water supply and streamflow trends in the Upper Colorado River Basin*, Lake Powell Research Project Bulletin No. 18: National Science Foundation, 70 pp.

Thompson, D.W.J. and Wallace, J.M. (2001) Regional climate impacts of the Northern Hemisphere Annular Mode. *Science*, 293, 85-89.